Geoscience Frontiers 16 (2025) 102148

Contents lists available at ScienceDirect

Geoscience Frontiers

journal homepage: www.elsevier.com/locate/gsf

Research Paper

Present-day temperature and pressure fields in key areas of Northeast China: Implications for unconventional resource evaluation

Yue Huang [a,b,c], Jian Chang [a,b,*], Nansheng Qiu [a,b], Nobuo Maeda [c]

[a] State Key Laboratory of Petroleum Resources and Engineering, China University of Petroleum (Beijing), Beijing 102249, China
[b] College of Geosciences, China University of Petroleum (Beijing), Beijing 102249, China
[c] Department of Civil and Environmental Engineering, School of Mining and Petroleum Engineering, University of Alberta, 7-207 Donadeo ICE, 9211-116 Street NW, Edmonton, AB, T6G1H9, Canada

ARTICLE INFO

Article history:
Received 7 May 2025
Revised 31 July 2025
Accepted 31 August 2025
Available online 4 September 2025

Keywords:
Temperature-pressure field
Gulong shale oil
Resource prediction
Resource evaluation
The Qingshankou Formation
Songliao Basin

ABSTRACT

The temperature-pressure fields within hydrocarbon-bearing basins are key geological factors controlling hydrocarbon generation, migration, and accumulation. In this study, we focus on the Qingshankou Formation in the northern part of the central depression of the Songliao Basin, China. A multi-parameter weighted evaluation model was created using present temperature-pressure field characteristics, with formation temperature-pressure as core variables, to evaluate shale oil resource potential. In addition, we explored the control mechanisms of temperature-pressure evolution during geological history on shale oil accumulation and further assessed the applicability of the proposed method. Our results show that the geothermal gradient of the Qingshankou Formation decreases from Member 1 to Member 3 (3.84 °C/100 m, 2.93 °C/100 m, and 2.49 °C/100 m, respectively). High-temperature zones are widely distributed in the Gulong sag, with the average temperature of the Gulong shale exceeding 95 °C and reaching an average of approximately 115 °C. Overpressure in the Qingshankou Formation exhibits a west-high to east-low trend. The overpressure zones of the Gulong shale are mainly concentrated in the Qijia-Gulong and Sanzhao sag, with average pressure coefficients of 1.52 and 1.36, respectively. The Opc model identified Class I and II favorable zones, mainly located in the central and southern parts of the Gulong Sag, as well as the central and southwestern Sanzhao Sag, with estimated shale oil resources of 7.1×10^8 tons and 17.2×10^8 tons, respectively. Evolutionary profiles from representative wells indicate that elevated temperatures enhance organic matter maturation and light oil generation, improving shale oil mobility, while overpressure suppresses hydrocarbon dissipation and provides a sufficient driving force for oil production. This study demonstrates that present-day temperature-pressure fields effectively reflect the evolution trends of paleo-thermal and pressure regimes. The proposed evaluation method shows strong applicability and scalability, offering a new technical framework and theoretical foundation for the exploration of unconventional hydrocarbon resources.

1. Introducton

Unconventional shale oil and gas resources are crucial in tackling the global energy crisis. As China's first shale oil demonstration site, the Gulong shale oil play in the Songliao Basin was estimated in 2021 to have geological resources of 12.68×10^8 t and proven reserves of 2.04×10^8 t. Characterized by in situ accumulation and high-light hydrocarbon content, it has become a key target for prioritized development (Cui et al., 2022, 2024; Meng et al., 2022, 2024). With ongoing exploration and production activities, the evaluation of shale oil resource potential has been steadily refined (Sorrell et al., 2010; McGlade, 2012; Cui et al., 2022; Sun et al., 2024). However, issues like production variability and spatial heterogeneity in hydrocarbon enrichment remain significant because of the complex geological settings and strong heterogeneity of shale reservoirs, creating major challenges for accurate resource prediction and evaluation (McGlade, 2012; Zhao et al., 2020a; Hu et al., 2022). Currently, mainstream techniques for predicting and evaluating shale oil and gas "sweet spots" include the comprehensive information superposition method (Jarvie, 2012; Zhao et al., 2020b; Li et al., 2022; Sun et al., 2023b; Cui et al., 2024), comprehensive evaluation index method (Zhao et al.,

* Corresponding author at: State Key Laboratory of Petroleum Resources and Engineering, China University of Petroleum (Beijing), Beijing 102249, China.
E-mail address: changjian@cup.edu.cn (J. Chang).

https://doi.org/10.1016/j.gsf.2025.102148

2020b; Zhou et al., 2020), weighted factor method (Zhang et al., 2019), and well-seismic integration method (Pan et al., 2018). These methods usually include parameters like porosity, oil saturation, organic matter quantity and maturity, shale thickness, oil content, and fracture development. However, a major shortcoming of existing studies is the common neglect of two key parameters—formation temperature and pressure, which are vital for hydrocarbon generation, migration, and preservation (Niu et al., 2022; Xu et al., 2022; Sun et al., 2023a). Omitting these factors can cause systematic bias in resource assessment and hinder a complete understanding of shale oil and gas potential (Dong et al., 2016; Niu et al., 2022; Yuan et al., 2023).

In recent years, advances in unconventional oil and gas exploration technologies have offered new insights into how shale oil and gas accumulate, mainly through studies of temperature and pressure (T-P) field distributions (Ma et al., 2017; Xin et al., 2019; Wang et al., 2023b). The T-P field not only explains the controls of subsurface thermal and pressure regimes on hydrocarbon generation, migration, and retention but also provides a scientific basis for precisely defining hydrocarbon enrichment zones (Sun et al., 2015; Qiu et al., 2018; Sun et al., 2021a; Zhang et al., 2022). Studies have shown that the T-P field directly influences the occurrence states of shale oil and gas; high-temperature and overpressure zones tend to exhibit a higher proportion of free hydrocarbons, enhanced fluidity, and increased reservoir mobilization potential (Wang, 2018). However, most current studies still regard the T-P field as a supplementary element in accumulation analysis or hydrocarbon migration modeling, without fully exploring its potential in quantitative resource evaluation. As a result, methodologies that incorporate T-P variables into resource assessment remain in the early exploratory stage (Jia and Pang, 2015; Sun et al., 2015, 2021b, 2023a; Qiu et al., 2018; Wang et al., 2022). At present, only the TSM basin modeling approach explicitly accounts for T-P field controls in determining the effective thickness and spatial extent of shale oil zones (Wang et al., 2022), while some laboratory-based methods have attempted to adjust adsorbed oil estimates using formation temperature and pressure constraints (Li et al., 2023a). Nevertheless, these approaches have not yet been practically adopted in real-world field development zones (Chen et al., 2019; Hu et al., 2021). Given that hydrocarbon mobility is a fundamental determinant of shale oil recoverability, the prediction of shale oil sweet spots should prioritize this aspect, with the T-P field serving as a dominant geological factor influencing hydrocarbon composition dynamics and ultimate recovery efficiency (Jarvie, 2012; Zhang et al., 2014; Yang et al., 2015; Lu et al., 2016; Akkutlu et al., 2017; Chen et al., 2019; Li et al., 2020; Wang et al., 2023b). High formation temperatures are essential for enhancing thermal maturity and hydrocarbon fluidity, while formation overpressure supplies the necessary driving force for mobilizing retained hydrocarbons, both serving as critical geodynamic controls on shale oil enrichment and production (Zou et al., 2016; Soeder, 2018; Wang et al., 2019b; Cui et al., 2020, 2024; Wei et al., 2021; Zhang, 2021; Zhao et al., 2023, 2024). Therefore, optimizing sweet spot prediction strategies based on T-P field characteristics represents an urgent and promising research frontier (Xu et al., 2022).

This study focuses on the Qingshankou Formation in the northern part of the Central Depression of the Songliao Basin. A total of 759 wells were analyzed using comprehensive well-logging data, including 211 wells with formation temperature measurements, 215 wells with drilling mud density data, and 279 wells with integrated well-logging datasets. Based on these data, the present-day temperature and pressure (T-P) field distribution across the study area was systematically characterized. A sensitivity analysis was then performed on key parameters, formation pressure, formation temperature, effective shale thickness, organic matter maturity (R_o), and oil production to establish a T-P field-based resource evaluation framework and assess the shale oil potential. On this basis, the study further investigates the differential enrichment mechanisms of shale oil under the control of the T-P field, and evaluates the applicability of the proposed method. The results underscore the critical role of the T-P field in governing shale oil enrichment patterns and guiding resource potential assessment.

2. Geological setting

The Songliao Basin is located in northeastern China. It is structurally divided into six first-order tectonic units: the Northern Subsidence Zone, Central Depression Zone, Northeastern Slope, Southeastern Uplift, Southwestern Uplift, and Western Slope (Fig. 1). The northern part of the Central Depression, bounded by the Songhua River in Zhaoyuan County, forms the main hydrocarbon-rich area of the Daqing Oilfield. This region trends northeast and can be subdivided into seven second-order structural units: the Heiyupao Sag, Mingshui Terrace, Longhupao-Da'an Terrace, Qijia-Gulong Sag, Daqing Placanticline, Sanzhao Sag, and Chaoyanggou Terrace (Liu et al., 2019; He et al., 2022). From the basin center to its margins, depositional environments transition from deep to semi-deep lacustrine facies into deltaic facies, displaying typical lacustrine sedimentary characteristics and complex hydrodynamic conditions (Sun et al., 2022, 2024; Wang et al., 2023a). During the depositional period of the Qingshankou Formation, the basin was in an expansive phase, marked by the continuous development of deep-water lacustrine sags (Chen et al., 2016; Kang et al., 2023). The formation exhibits a variable thickness ranging from 20 to 550 m, with lithologies primarily consisting of black and gray shales interbedded with oil shales, siltstones, and thin ostracod limestones. Locally, fine sandstones and thin-layered siltstones are also developed. The sediments are rich in microfossils such as ostracods, conchostracans, and bivalves (Wang et al., 2019a; He et al., 2021; Bai et al., 2024).

A wide maturity range and high-quality kerogen characterize the Gulong Shale within the Qingshankou Formation. Vitrinite reflectance (R_o) values range from 0.5% to 1.7%, and the organic matter is predominantly composed of Type I and Type II_1 kerogen, indicating strong hydrocarbon generation potential (Liu et al., 2023b). Regional tectonic activity and depositional variations have resulted in significant spatial heterogeneity in shale thickness and T-P field conditions. The basin center, in particular, is characterized by thicker shale sequences and elevated formation temperatures and pressures, creating favorable conditions for hydrocarbon generation, accumulation, and preservation (Zheng et al., 2009; Qiu et al., 2018; Ren et al., 2020; Lu et al., 2024). These geological and geochemical characteristics provide a solid foundation for evaluating shale oil potential in the Qingshankou Formation and offer necessary guidance for future exploration strategies.

3. Evaluation parameter data acquisition and methodology

3.1. Effective data screening for Qingshankou Formation shale thickness

The thickness of shale in the Qingshankou Formation within the Central Depression exhibits a decreasing trend from west to east and from south to north. This formation is characterized by substantial thickness, strong heterogeneity, and a shale content exceeding 95% (Sun et al., 2021a, 2023a; Wang et al., 2021; Li et al., 2022). Previous studies have suggested that a TOC value above 1.0% serves as the lower threshold for evaluating shale oil resources in the Qingshankou Formation (Sun et al., 2024), and that when TOC exceeds 2.0% in continental shale reservoirs, both the

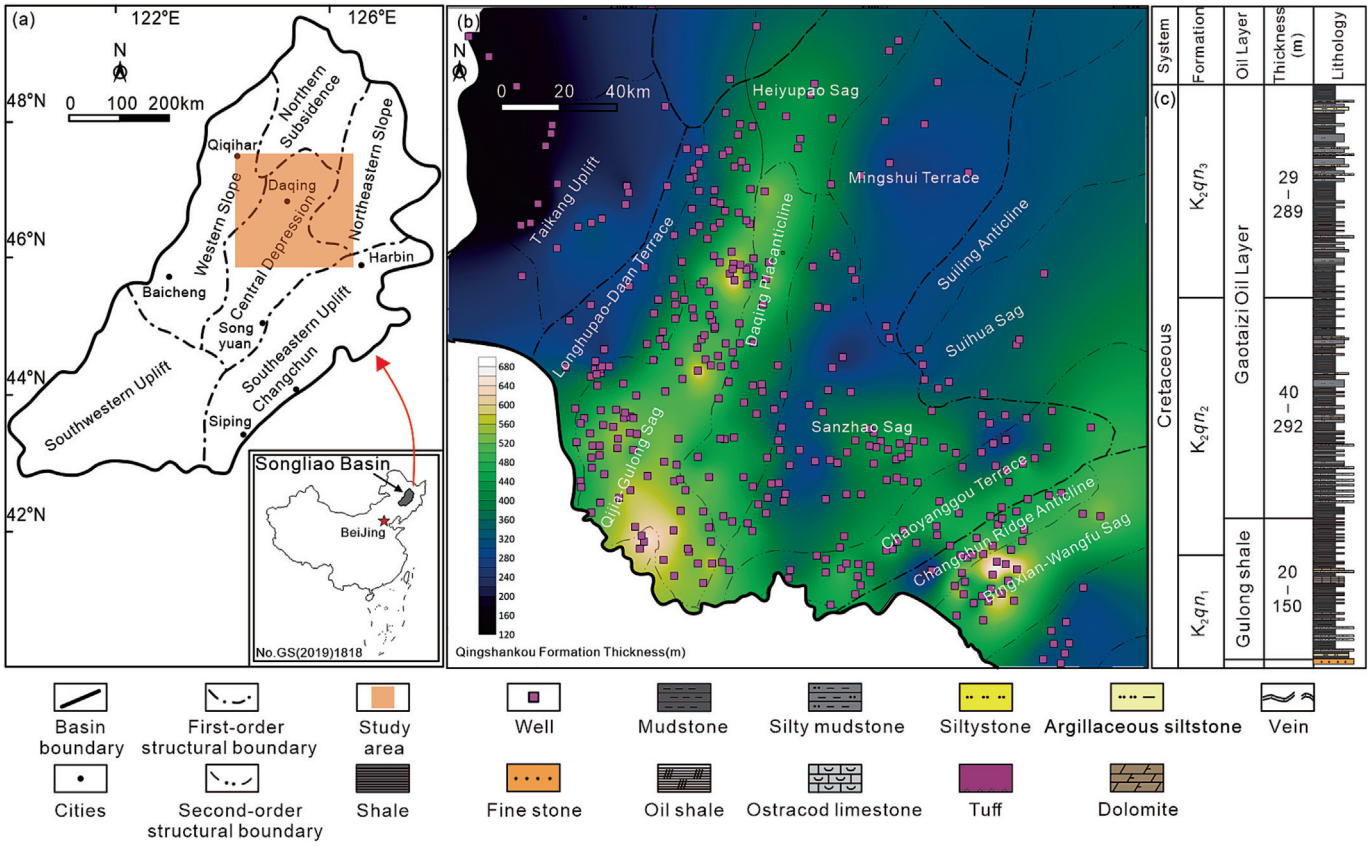

Fig. 1. (a) Location of the Songliao Basin. (b) Location of the Central Depression in the Songliao Basin and the Qingshankou Formation thickness. (c) Stratigraphic and lithological characteristics of the Qingshankou Formation in the study area. (Note: this study label "Gulong Shale" refers only to the Gulong shale interval within the Qingshankou Formation, specifically Member 1 and the base of Member 2; it does not include Members 1 and 2 of the Nenjiang Formation.)

quantity of retained hydrocarbons and the frequency of high movable oil index values increase significantly (Zhao et al., 2023). Accordingly, in this study, high-organic carbon content shale intervals are used to define effective shale. Due to limited core data, accurately determining the spatial distribution of effective shale thickness is challenging. However, compared to other lithologies, shale exhibits distinctive responses in well-logging parameters, which allow for accurate identification and estimation of thickness and vertical characteristics based on well-log data and curve interpretation (Chen, 1996; Hao et al., 2012; Chen et al., 2016; Li et al., 2020; Tan et al., 2021).

The Qingshankou Formation shale generally exhibits higher values of natural gamma-ray (GR) and sonic transit time (t) compared to other lithologies (Wang et al., 2021). Based on a comparison between single-well lithological descriptions and well-log data, intervals with t > 90 s/ft, GR > 120 API, and estimated TOC > 2% (calculated via the $\Delta \log R$ method) were identified as effective shale layers (Fig. 2) (Huang et al., 2024). To reduce manual interpretation errors, a Python-based program was developed to automatically extract the thickness of high-organic matter intervals in different submembers of the Qingshankou Formation and the Gulong shale. Data quality was further ensured through multiple rounds of cross-validation and geological consistency checks. Effective shale intervals were calibrated using integrated well-log data. For example, in Well X23, the well-logs result thickness of high-organic matter shale was 119.8 m, while the processed result was 117.9 m, corresponding to an absolute error of 1.9% (Fig. 2a and Fig. 3). Similarly, in Well J54, the measured thickness was 56.2 m, and the processed result was 54.5 m, with an absolute error of 1.7% (Fig. 2b and Fig. 3). This rigorous data acquisition and processing workflow provides a robust foundation for subsequent resource evaluation and the delineation of favorable shale oil zones in the Qingshankou Formation.

3.2. Screening of present-day geothermal field data

A total of 211 wells with well-logging temperature data and 512 steady-state formation temperature measurements from oil testing were collected, including data from 12 horizontal wells targeting the Gulong shale. For each well, stratified data from submembers of the Qingshankou Formation were filtered using Python scripts. Duplicate entries and anomalous temperature points were removed to ensure data quality. The arithmetic mean of temperature values within the corresponding depth interval was calculated to represent the formation temperature of each submember. Additionally, geothermal gradients (GG) were derived based on these intervals. The calculation method for GG is shown in Eq. (1).

$$GG = \frac{T_{\text{bottom}} - T_{\text{top}}}{D} \tag{1}$$

In Eq. (1), T_{bottom} represents the temperature at the bottom of the formation, T_{top} denotes the temperature at the top, and D is the thickness of the formation. GG stands for the geothermal gradient, calculated as the temperature difference per unit thickness.

Since well-log temperature (*log temperature*) does not typically represent the accurate formation equilibrium temperature, it must be corrected to reflect in situ thermal conditions accurately. During the logging process, the fluid temperature inside the borehole is influenced by the circulation of drilling mud, resulting in a mea-

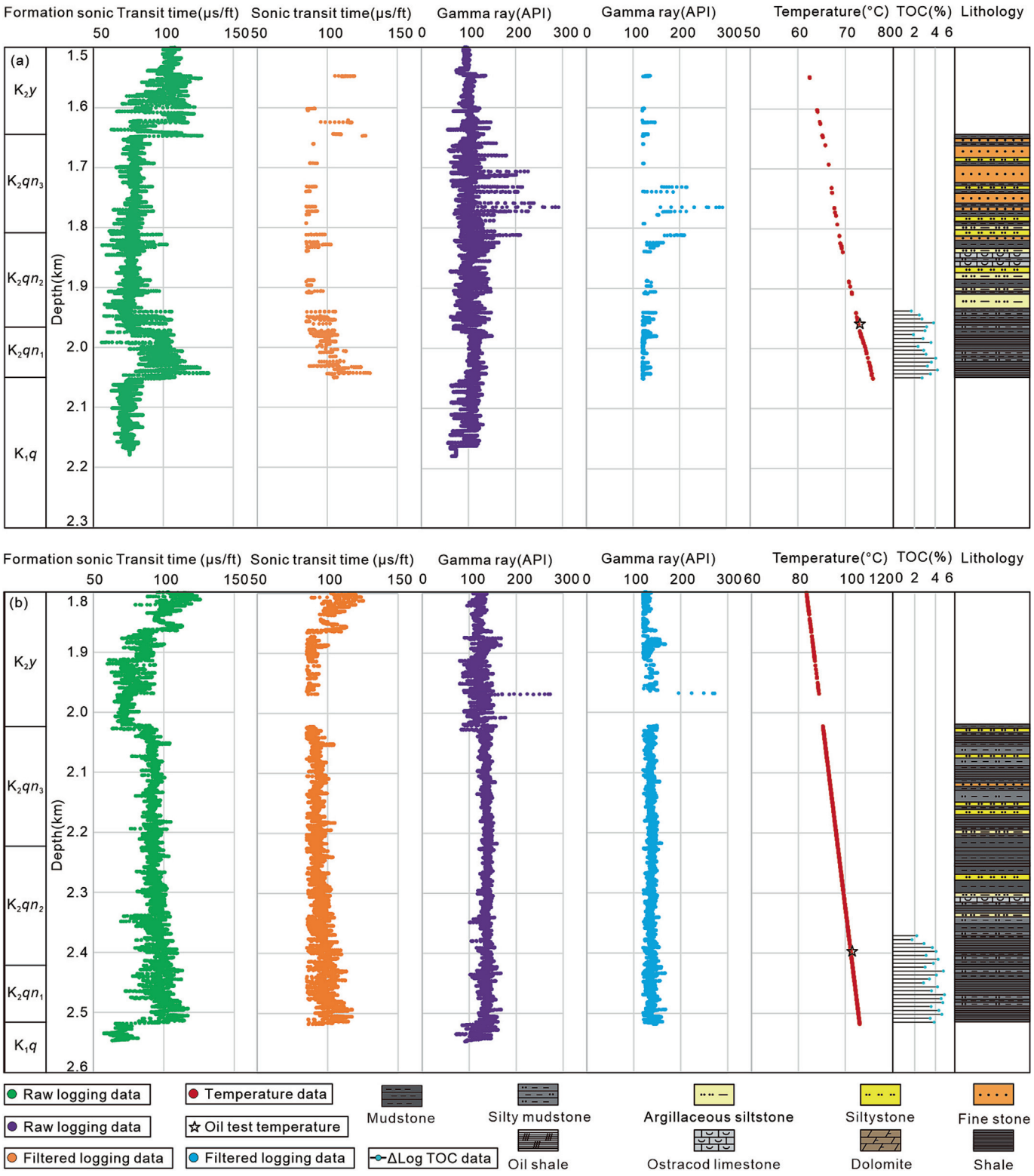

Fig. 2. Shale data screening results for (a) Well J54 and (b) Well X23.

sured temperature that is lower than the actual formation temperature. Therefore, log temperature is essentially a transient value and requires correction to approximate the steady-state formation temperature. In this study, multiple temperature measurements were taken at the same stratigraphic level across different time intervals. The correction was performed using the Bullard extrapolation method, which is widely adopted to estimate the accurate formation equilibrium temperature (Bullard, 1939; Lin et al., 2023). The correction formula is provided in Eq. (2).

$$T_f = T_m + S \cdot t^{-0.5} \tag{2}$$

To accurately correct well-log temperature data to reflect the formation equilibrium temperature, an empirical coefficient (S) is

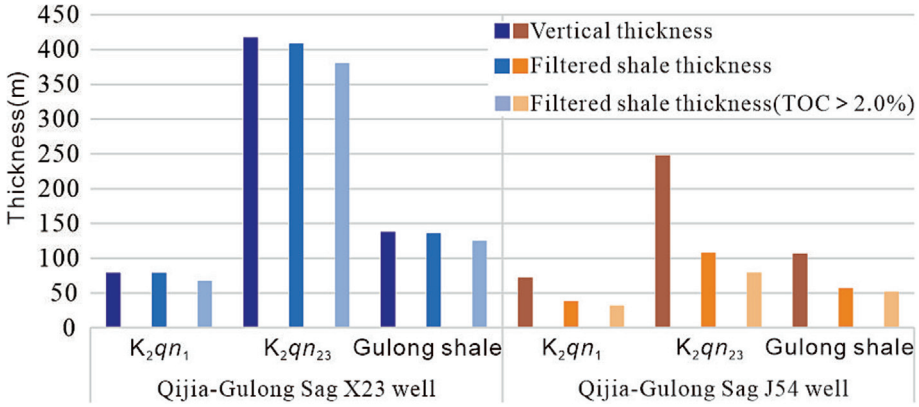

Fig. 3. Comparison of total formation thickness and effective shale thickness for different subunits of the Qingshankou Formation in representative wells.

introduced. Fitting formation testing temperature data with corresponding well-log temperature measurements from the same stratigraphic level derive this coefficient. The correction formula incorporates the measurement time (t, in hours) and the instantaneous well-log temperature (T_m) recorded at multiple time points. The empirical coefficient S varies across the sub-members of the Qingshankou Formation: it ranges from 1.28 to 1.13 in the Qing 1 Member, 1.07 to 1.15 in the Qing 2 Member, and 1.02 to 1.09 in the Qing 3 Member. The measurement time t is calculated based on the logging speed. This parameterization ensures that the corrected temperatures are stratigraphically consistent and representative of the actual formation conditions.

To verify the reliability of the corrected data, a well-by-well comparison was conducted between the processed well-log temperature data, formation equilibrium temperatures obtained from oil testing, and temperature logging data from horizontal wells at corresponding stratigraphic levels. The results show that the absolute error among the three datasets is within 3%, confirming that the corrected well-log temperatures provide a reliable representation of formation temperatures in the Qingshankou Formation (Fig. 2).

3.3. Acquisition of present-day formation pressure field data

In this study, a total of 137 drill stem test (DST) pressure measurements from 97 wells, three modular formation dynamics test (MDT) pressure data from 3 wells, mud density records from 375 wells, and integrated well-logging data from 338 wells were collected in the Central Depression of the Songliao Basin.

However, the measured pressure datasets present two primary limitations:

(1) The sample size is insufficient for regional characterization. Only 41 pressure measurements are available for the Qing 1 Member, while the 96 pressure points for the Qing 2 and Qing 3 Members are heavily concentrated in the Qijia-Gulong Sag, which limits their representativeness for the entire Central Depression.

(2) The DST-derived pressures mainly reflect formation pressure in permeable zones. Given the low porosity and permeability of shale formations, acquiring representative formation pressure data directly from shale intervals remains challenging.

To more comprehensively delineate the formation pressure distribution within the Qingshankou Formation's shale intervals, this study employed Eaton's method (Eaton, 1975; Zhang et al., 2024) using mud weight data from 375 wells and complementary well-logging responses from 338 wells. This approach integrates measured mud density and resistivity logs to calculate the composite formation pressure, which is especially useful in low-permeability shale intervals. The Eaton pressure estimation formula is given in Eq. (3).

$$P_P = P_V - \left[(P_V - P_N) \left(\frac{\Delta t_n}{\Delta t_s} \right)^C \right] \quad (3)$$

In the Equation, P_V represents the overburden pressure in MPa; P_N is the normal pore pressure in MPa; Δt_n is the sonic transit time under normal compaction conditions; Δt_s is the actual sonic transit time at the same depth; and C is the Eaton exponent, with a value range of 0.32–0.96 for the study area.

To validate the predictive performance of the formation pressure model, two wells, X33 and J43, were selected for comparison between measured and predicted formation pressures. In Well X33, at a depth of 2209.2 m, the measured formation pressure in the shale interval was 33.1 MPa, while the predicted pressure was 31.4 MPa, yielding a relative error of 5.14% and a pressure coefficient of 1.54 (Fig. 4a and Fig. 4b). In Well J43, at a depth of 2120.3 m, the measured pressure was 22.8 MPa, and the predicted pressure was 21.2 MPa, with a relative error of 7.02% (Fig. 4a and Fig. 4b). Overall, the relative errors between measured and predicted formation pressures remained within ± 3 MPa, indicating a high degree of reliability in the pressure prediction results (Fig. 4).

It is worth noting that mud density is generally designed to exceed actual pore pressure to ensure drilling safety. Therefore, in this study, mud density was not used as a direct indicator of formation pore pressure. Instead, it served to constrain the general pressure trend and provided auxiliary guidance for identifying potential overpressure zones, particularly in data-sparse regions.

3.4. Methodology

Integrating well-logging data and core data to predict shale oil sweet spots significantly enhances the accuracy of identification (Niu et al., 2022; Cao et al., 2024). This study establishes a comprehensive resource evaluation framework and investigates the shale oil enrichment mechanisms controlled by the coupling effects of temperature and pressure (T-P) fields (Fig. 5). The methodological workflow comprises the following steps: (i) Comprehensive datasets were collected from the study area, including well-logging and mud-logging data, measured formation pressures, formation temperatures from well testing, single-well shale oil production volumes, and geochemical parameters. (ii) Key evaluation parameters such as formation pressure and formation temperature for each sub-member of the Qingshankou Formation and the Gulong Shale were defined (see Section 3.2 and Section 3.3). (iii) The spatial distribution patterns of each evaluation parameter were mapped across the Qingshankou Formation and Gulong Shale

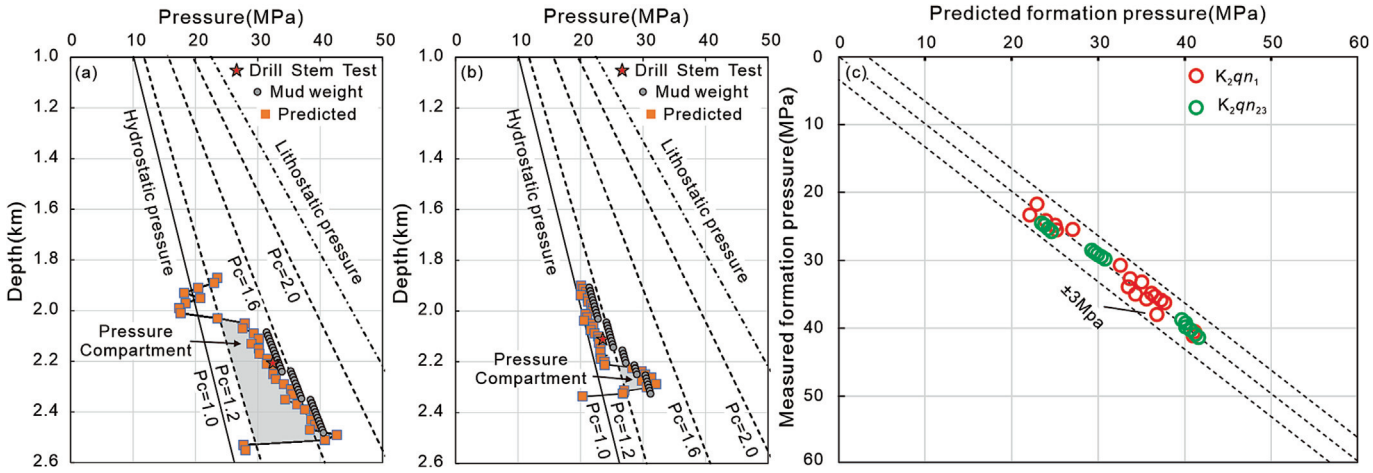

Fig. 4. Comparison between measured and predicted formation pressures: (a) Well X33, (b) Well J43, and (c) all measured data points combined.

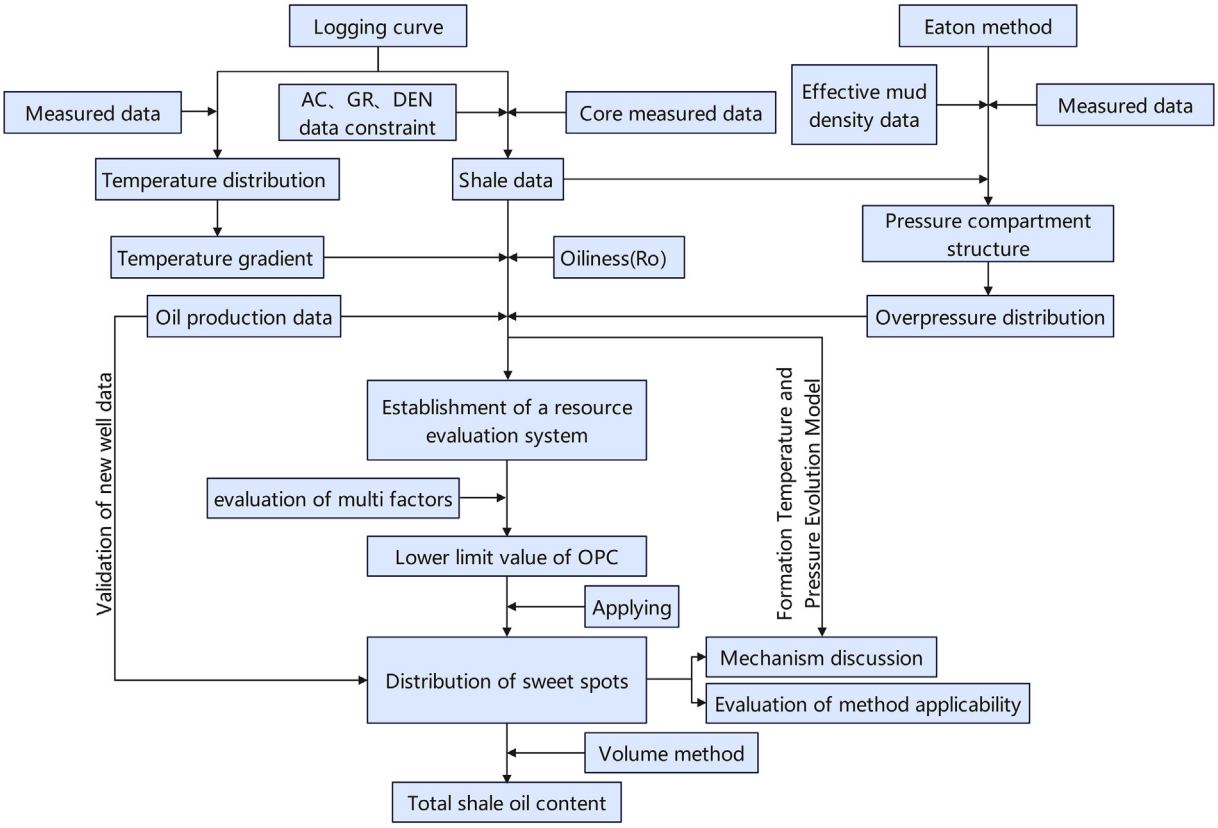

Fig. 5. Illustrates the methodological framework of this research.

intervals. (iv) Based on the correlations among shale thickness, vitrinite reflectance (R_o), oil content (S_1), and shale oil production, Pearson correlation coefficients were calculated to quantify the contribution of each parameter. These coefficients were used as weighting factors to construct a shale oil resource evaluation model controlled by T-P fields. (v) Weighted overlay analysis was applied to classify favorable shale oil development zones and delineate enrichment areas. The Output coefficient (Opc) was introduced to quantify the relationship between geological resource abundance and actual hydrocarbon enrichment levels. (vi) A volumetric method based on small-scale grid units was employed to conduct a tiered assessment of shale oil resource potential across different zones. (vii) Finally, the differential enrichment mechanisms of shale oil under the influence of T-P field coupling were analyzed, and the applicability of this method was discussed.

4. Results

4.1. Hydrocarbon source rock characteristics of shales in the Qingshankou Formation

In shale oil resource evaluation, vitrinite reflectance (R_o) is a key parameter that reflects the thermal maturity of organic matter and

plays a crucial role in assessing the potential of shale oil resources (Guo et al., 2021; Sun et al., 2024). In this study, a total of 1,083 R_o measurements were collected from the Gulong Shale in the northern part of the Central Depression. Based on this dataset, the spatial distribution characteristics of R_o across the Qingshankou Formation were systematically analyzed (Fig. 6).

The R_o dataset compiled in this study includes measurements from 232 wells for the first member of the Qingshankou Formation, 78 wells for the second member, and 59 wells for the third member. The results show that R_o values increase with burial depth. In the first member, extensive high R_o zones (>1.2) are observed (Fig. 6a), with R_o values reaching 1.67 and 1.72 in Wells X1 and X12, respectively. Spatially, these high-value zones are mainly distributed in the Qijia-Gulong Sag and the central part of the Sanzhao Sag. Within the Qijia-Gulong Sag, R_o values greater than 1.2 are primarily concentrated in the southern Qijia Sag and the central Gulong Sag, whereas both the maximum R_o values and their distribution range in the Sanzhao Sag are lower than those in the Qijia-Gulong Sag (Fig. 6a–c).

Overall, the high R_o zones are predominantly concentrated in the Qijia-Gulong Sag, followed by the central area of the Sanzhao Sag. This distribution indicates that these regions possess favorable conditions for hydrocarbon generation and preservation, representing advantageous zones for potential shale oil enrichment.

4.2. Distribution characteristics of effective shale thickness in the Qingshankou Formation

The thickness of shale in the Qingshankou Formation is a key parameter for evaluating shale oil resources. Based on well-logging data and stratigraphic division information (see Section 2), this study constructed vertical thickness maps for the first member, the combined second and third members, and the Gulong shale, including both total thickness and black shale thickness (Fig. 1b), to accurately assess the development of effective black shale.

The results show that in the northern part of the Central Depression, the total thickness of the Qingshankou Formation ranges from 130 m to 680 m, while the shale thickness varies from 20 m to 550 m (Fig. 1b). Further analysis indicates the following:

(1) The total thickness of the first member ranges from 20 m to 150 m, with shale thickness between 4 m and 143 m (Fig. 7a and b);

(2) The combined second and third members have total thicknesses ranging from 80 m to 590 m, with shale thickness between 2 m and 465 m (Fig. 7c and d);

(3) The total thickness of the Gulong shale ranges from 40 m to 200 m, and its shale thickness spans 28 m to 187 m (Fig. 7e and f).

Overall, the proportion of shale in Member 1 of the Qingshankou Formation ranges from 92.8% to 98.5%, while in Members 2–3 it ranges from 22.3% to 98.2%. The Gulong shale shows a shale proportion ranging from 77.3% to 96.5%. In terms of spatial distribution, the thickness of black shale generally shows a pattern of "thinner in the east, thicker in the west and southeast" reflecting the combined effects of depositional environments and tectonic activities (Li et al., 2017; Liu et al., 2018). The areas with greater thickness are mainly concentrated in the Qijia-Gulong Sag.

Within the key study area of the Qijia-Gulong Sag, the thick black shale intervals in Member 1 of the Qingshankou Formation and the Gulong shale are mainly distributed in the southern Qijia Sag and the central Gulong Sag (Fig. 7a, b, e and f). In contrast, the thicker pure shale zones of Members 2 and 3 are concentrated

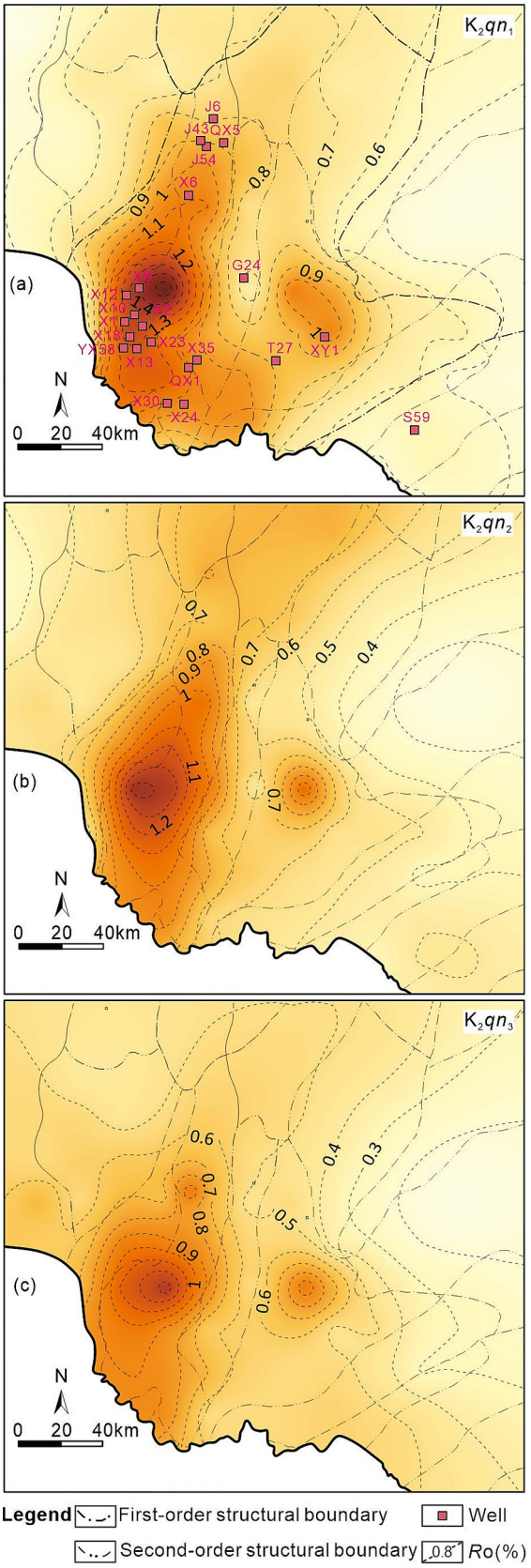

Fig. 6. Contour maps of vitrinite reflectance (R_o(%)) for the Qingshankou Formation: (a) Member 1, (b) Member 2, and (c) Member 3.

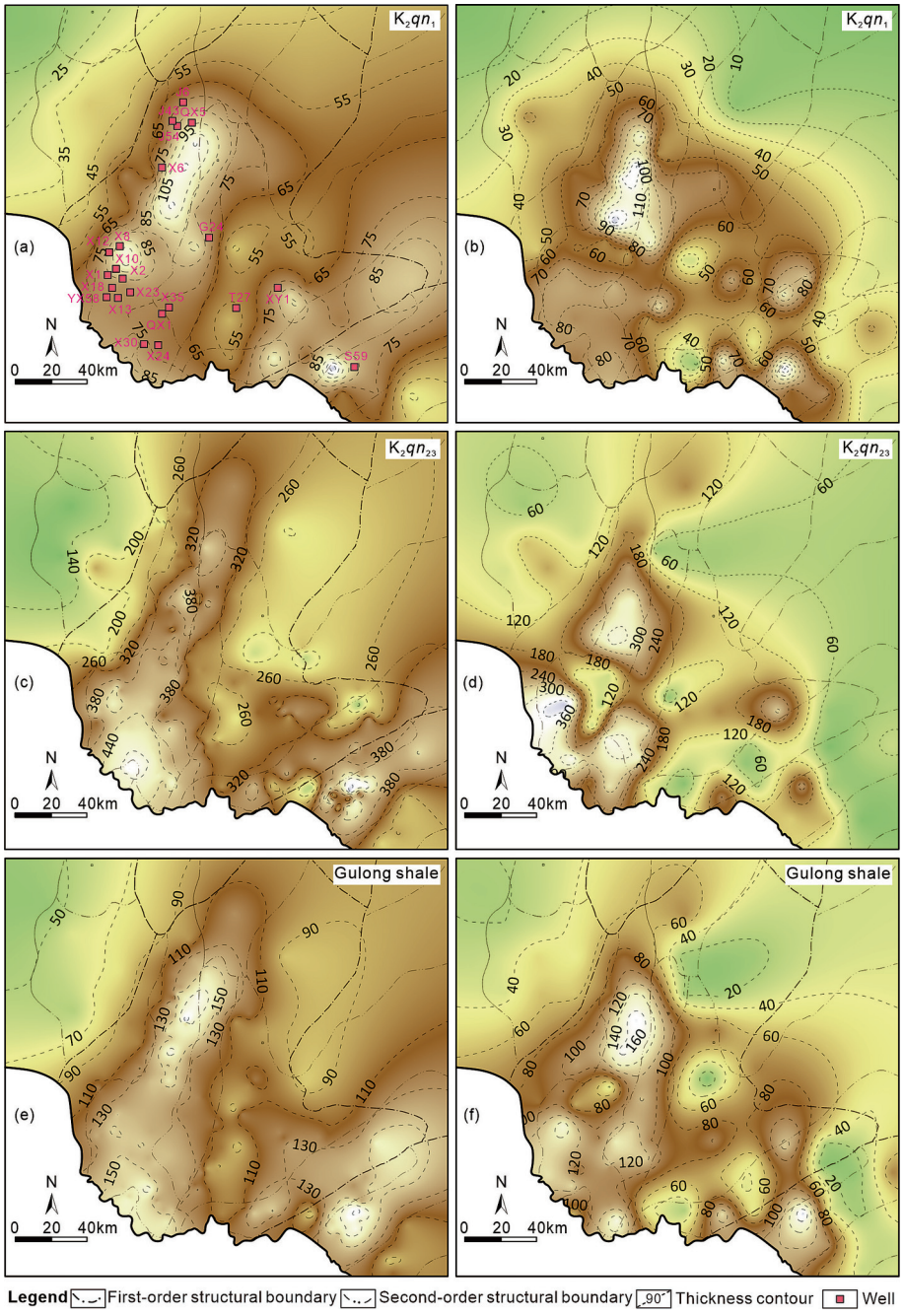

Fig. 7. Contour maps of vertical thickness and shale thickness for different intervals: (a–b) Member 1 of the Qingshankou Formation, (c–d) Members 2–3 of the Qingshankou Formation, and (e–f) the Gulong shale.

in the southern part of the Qijia Sag, the central Gulong Sag, and the south section of the Daqing-Changyuan Uplift (Fig. 7c and d). Notably, thinning zones of black shale are observed in the northern and northeastern Gulong Sag (Fig. 7), indicating a mismatch between the total formation thickness and that of black shale. This suggests the possible predominance of interbedded type shale oil reservoirs in this area.

4.3. Present-day temperature field distribution characteristics

The present-day formation temperature distribution of the Qingshankou Formation in the northern Central Depression of the Songliao Basin shows that high-temperature zones are predominantly located in the Qijia-Gulong Sag, particularly within the central part of the sag. The formation temperatures of Member 1, Member 2, and the Gulong shale are generally above 90 °C, with the Gulong shale in the central Gulong Sag exhibiting an average formation temperature of 115 °C. Notably, the maximum temperature in Member 1 reaches 121 °C, which corresponds to the average formation temperature over a 2.5 km horizontal section of the X10 well. Different subunits of the Qingshankou Formation exhibit distinct temperature ranges based on well-log temperature measurements: Member 1 ranges from 33.7 °C to 121.3 °C, Member 2 from 26.1 °C to 111.2 °C, and Member 3 from 24.5 °C to 105.2 °C (Fig. 8).

Regionally, the formation temperature distribution exhibits a distinct east-west contrast. In the eastern Sanzhao Sag, the formation temperature of the Gulong shale is relatively low, ranging

from 61.2 °C to 82.3 °C, while in the western Qijia-Gulong Sag, the temperature is significantly higher, ranging from 63.4 °C to 121.3 °C. Within the Qijia-Gulong Sag, there is also a clear north-south temperature differentiation: the central part of the southern Gulong Sag shows elevated formation temperatures between 83.2 °C and 121.3 °C, whereas the Gulong shale in the northern Qijia Sag records lower values, ranging from 63.4 °C to 73.8 °C. These spatial differences reflect the strong influence of regional tectonic activity and heat flow background on the present-day thermal regime. Such variations offer critical insights into the thermal evolution of the Qingshankou Formation, hydrocarbon accumulation patterns, and shale oil resource evaluation.

The geothermal gradient of the Qingshankou Formation and Gulong Shale exhibits significant variations across different subunits. Member 1 of the Qingshankou Formation has an average geothermal gradient of 3.84 °C/100 m, with the highest value recorded at Well X35 (9.6 °C/100 m) and the lowest at Well X10 (0.5 °C/100 m). Member 2 shows an average geothermal gradient of 2.93 °C/100 m, with a maximum value of 6.38 °C/100 m at Well X2 and a minimum of 0.35 °C/100 m at Well S59. Similarly, Member 3 presents an average geothermal gradient of 2.49 °C/100 m, with the highest value of 4.92 °C/100 m at Well T27 and the lowest of 1.1 °C/100 m at Well G24. The Gulong shale demonstrates an average geothermal gradient of 3.6 °C/100 m, with the highest recorded value at Well YX58 (7.4 °C/100 m) and the lowest at Well S59 (0.49 °C/100 m). Regionally, within the Gulong shale interval, the average geothermal gradients are observed in the Qijia-Gulong Sag (4.43 °C/100 m) and the Longhupao-Da'an Platform (4.12 °C/100 m) (Fig. 9). These variations in geothermal gradient reflect the influence of regional tectonic activity and heat flow distribution, which play a crucial role in controlling the thermal evolution and hydrocarbon generation potential of the Qingshankou Formation.

4.4. Present-day pressure field distribution characteristics

The formation pressure of the Qingshankou Formation in the northern Central Depression of the Songliao Basin generally increases with burial depth, with pressure progressively rising from Member 3 to Member 2 and reaching its highest levels in Member 1. The overpressure distribution within the Qingshankou Formation varies across different secondary structural units. Significant overpressure is observed in the Longhupao-Daan Terrace, Qijia-Gulong Sag, Daqing Placanticline, and Sanzhao Sag. Among these, the most extensive overpressure zones are primarily located in the central Sanzhao Sag and the Qijia-Gulong Sag (Fig. 10 and Fig. 11).

The formation pressure coefficients of the Qingshankou Formation exhibit significant variations in both stratigraphy and space. Specifically, Member 3 shows pressure coefficients ranging from 0.78 to 1.43 (Fig. 11a); Member 2 ranges from 0.81 to 1.67 (Fig. 11b); and Member 1 exhibits the highest values, ranging from 0.83 to 1.83 (Fig. 11c). For the Gulong shale, pressure coefficients in the central Sanzhao Sag range from 0.83 to 1.68 (Fig. 11d), while in the Qijia-Gulong Sag, they range from 0.82 to 1.83. Overall, formation pressures in the Qijia-Gulong Sag are consistently higher than those in the central Sanzhao Sag, highlighting the significant influence of regional tectonic activity and geological conditions on pressure distribution. These findings provide a critical foundation for further investigation into the pressure evolution of the Qing-

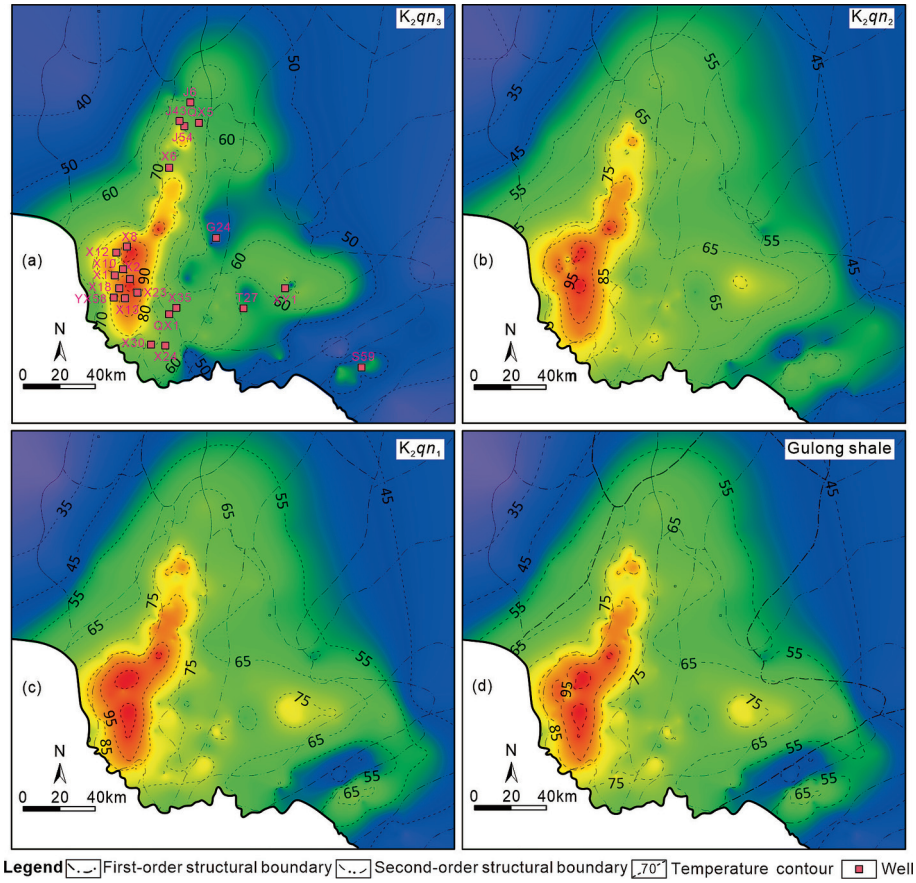

Fig. 8. Fig. 8. Contour maps of formation temperature for different intervals: (a) Member 3, (b) Member 2, (c) Member 1 of the Qingshankou Formation, and (d) the Gulong shale.

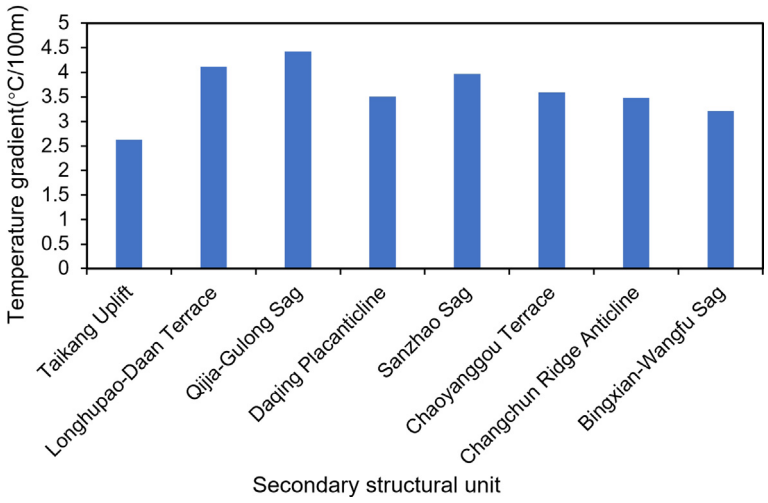

Fig. 9. Average geothermal gradient distribution map of the Gulong shale interval in different secondary structural units of Northern Songliao Basin.

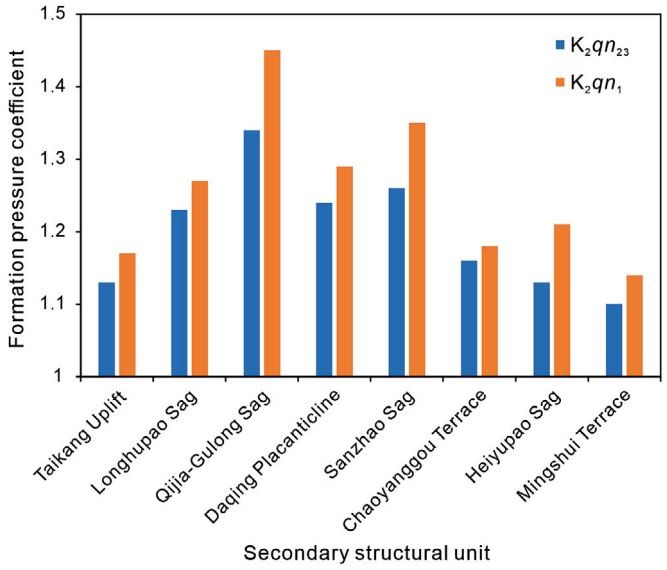

Fig. 10. Average formation pressure coefficient of the Qingshankou Formation in different secondary structural units of the northern Songliao Basin.

shankou Formation and its role in the accumulation of shale oil and gas.

4.5. Establishing an evaluation parameter system and model for the Gulong shales

The shale oil production of wells in the study area reflects the integrated influence of shale geological conditions. This study analyzes production data from 53 Qingshankou Formation Gulong shale oil wells. The average daily oil production is calculated based on the mean output over 120 days following initial well testing. Furthermore, correlations between key evaluation parameters effective shale thickness, vitrinite reflectance (R_o), formation pressure coefficient, and formation temperature and oil production were examined (Fig. 12).

The relationships between key evaluation parameters and shale oil production are summarized in Fig. 13. The thickness of the Gulong shale ranges from 70 to 110 m, and overall, production increases with thickness. Notably, when the thickness exceeds 90 m, daily oil production typically surpasses 20 t/d, indicating that formation thickness is a critical control on shale oil enrichment and serves as a key parameter for selecting favorable zones. Vitrinite reflectance (R_o) above 0.9 is associated with a marked increase in production. When R_o exceeds 1.3, maximum daily production can exceed 30 t/d, suggesting that appropriate R_o values are strong indicators of organic maturity and enrichment potential. Formation pressure coefficients ranging from 1.2 to 1.8 show a positive correlation with production, peaking around 1.6, which highlights the role of overpressure as a key geological control on shale oil enrichment. Similarly, formation temperatures between 70 °C and 110 °C show a general positive trend with productivity. In particular, temperatures in the range of 90–110 °C correspond to higher shale oil yields, underscoring that temperature governs the geochemical processes of hydrocarbon generation and is thus a crucial parameter in delineating sweet spot zones.

The classification thresholds for each evaluation parameter were independently determined based on their respective statistical distributions, and the delineated shale oil enrichment zones were used as input variables for the resource evaluation model. As summarized in Table A.1, these favorable zones were graded into four levels: Class I (highest priority), Class II, Class III, and Class IV (lowest priority). Areas with shale thickness > 90 m, pressure coefficient (P_c) >1.4, vitrinite reflectance (R_o) >1.2, and formation temperature between 90–110 °C were identified as having the most significant potential for shale oil enrichment. The evaluation results indicate that the Gulong shale in the central Gulong Sag represents a Class I favorable zone. At the same time, Members 2 and 3 of the Qingshankou Formation are classified as Class II favorable zones. The central Sanzhao Sag and the southern Daqing Placanticline are categorized as Class II to Class III favorable zones. This classification framework provides a scientific basis for prioritizing and categorizing productive shale intervals in the Gulong area, offering practical guidance for shale oil exploration and development.

To quantitatively assess the contribution of each parameter to shale oil enrichment, common methods include the Pearson weighting method, entropy weight method, analytic hierarchy process (AHP), and grey relational analysis. However, to better reflect productivity response and minimize subjective bias, this study adopts Pearson correlation analysis based on parameter classification and variation trends (Eq. (4)). The Pearson correlation coefficient evaluates the strength and direction of a linear relationship between two variables, ranging from −1 to 1, with values closer to the extremes indicating stronger correlation. Based on Pearson

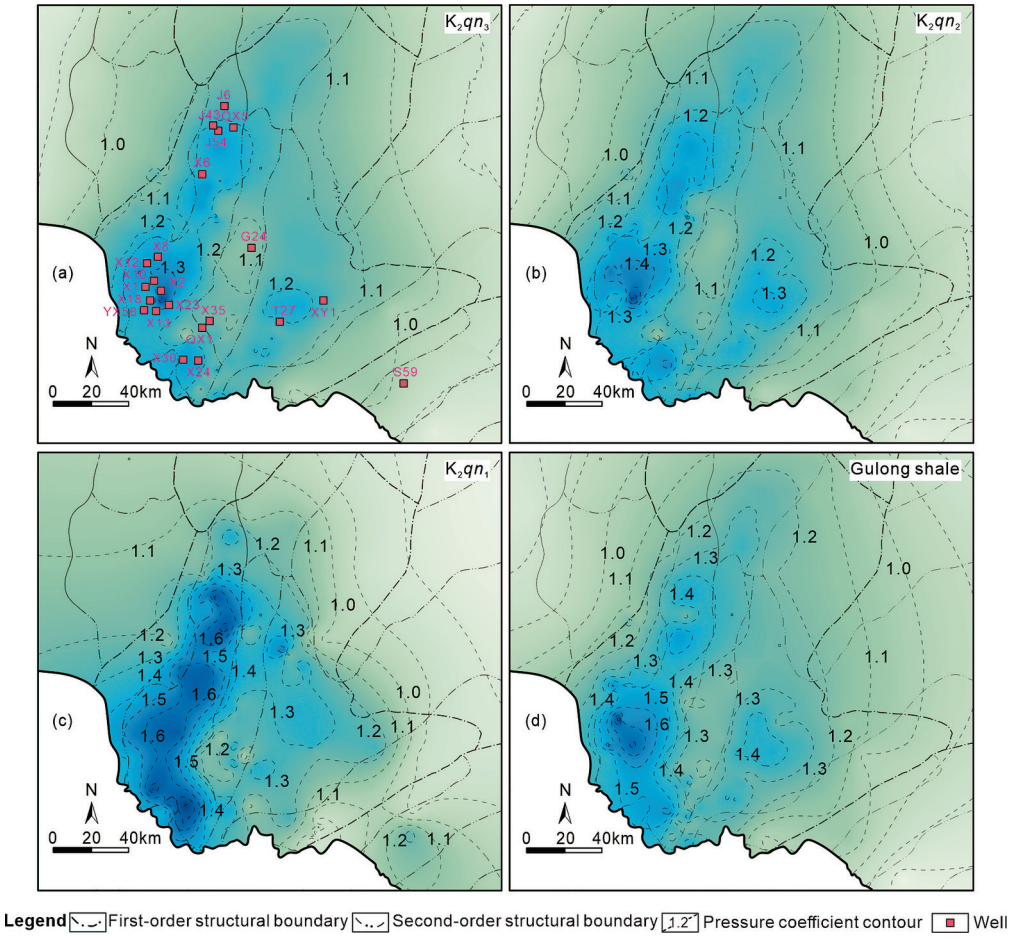

Fig. 11. Contour maps of formation pressure for different intervals: (a) Member 3, (b) Member 2, (c) Member 1 of the Qingshankou Formation, and (d) the Gulong shale.

correlation coefficients between shale oil production and pressure coefficient (P_c), formation temperature (T), vitrinite reflectance (R_o), and shale thickness, the resulting parameter weights were 0.29 for pressure, 0.27 for temperature, 0.29 for R_o, and 0.15 for shale thickness (Fig. 13). Although the correlation between thickness and production is lower than that of R_o or pressure, thickness still plays a crucial role in defining the resource enriched volume.

$$\gamma_{XY} = \frac{\sum_{i}^{n}(x_i - \overline{x})(y_i - \overline{y})}{\sqrt{\sum_{i}^{n}(x_i - \overline{x})^2}\sqrt{\sum_{i}^{n}(y_i - \overline{y})^2}} \tag{4}$$

x_i and y_i represent the observed values of oil production and the corresponding evaluation parameter for the i-th well, respectively. $\overline{x}$ and $\overline{y}$ denote the mean values of x and y within the sample dataset.

An integrated evaluation model was established by defining an output coefficient (Opc), which represents the potential productivity of shale oil. This coefficient is derived from a multi-factor weighted summation, where parameter weights are normalized using Pearson correlation coefficients. This approach ensures that the contribution of each variable is based on statistical correlation rather than subjective assignment, enhancing objectivity. To minimize the impact of extreme outliers on normalization, two preprocessing measures were implemented: (1) each parameter distribution was truncated within the P5–P95 percentile range to remove values that deviate significantly from the primary data trend; (2) the truncated data were then linearly normalized to ensure robustness. The formulation of the comprehensive evaluation model is as follows (Eq. (5)):

$$\begin{aligned}\mathrm{Opc} = {} & 0.29 \times \frac{a - a_{\min}}{a_{\max} - a_{\min}} + 0.27 \times \frac{b - b_{\min}}{b_{\max} - b_{\min}} \\ & + 0.29 \times \frac{c - c_{\min}}{c_{\max} - c_{\min}} + 0.15 \times \frac{d - d_{\min-\mathrm{eff}}}{d_{\max-\mathrm{eff}} - d_{\min-\mathrm{eff}}}\end{aligned} \tag{5}$$

In this equation, a denotes the formation pressure, b the formation temperature, c the vitrinite reflectance (R_o), and d the shale thickness. $d_{\min-\mathrm{eff}}$ and $d_{\max-\mathrm{eff}}$ represent the minimum and maximum effective shale thickness, respectively.

It is essential to note that the Opc index primarily reflects the geological potential for resource enrichment and does not incorporate engineering factors, such as the scale of fracturing or completion methods. Therefore, it cannot be used directly for production prediction. Although high Opc values do not necessarily correspond to high productivity, the correlation between Opc and oil production equivalents can serve as a supplementary indicator for validating the reliability of the geological model (Fig. 13). Based on Opc values, the favorable shale oil zones are classified into four categories (Table A.2): Class IV (<0.4), Class III (0.4–0.5), Class II (0.5–0.7), and Class I (>0.7). This model enables the quantitative characterization of shale oil enrichment potential, providing a robust geological foundation for the efficient development of the Gulong shale oil resource.

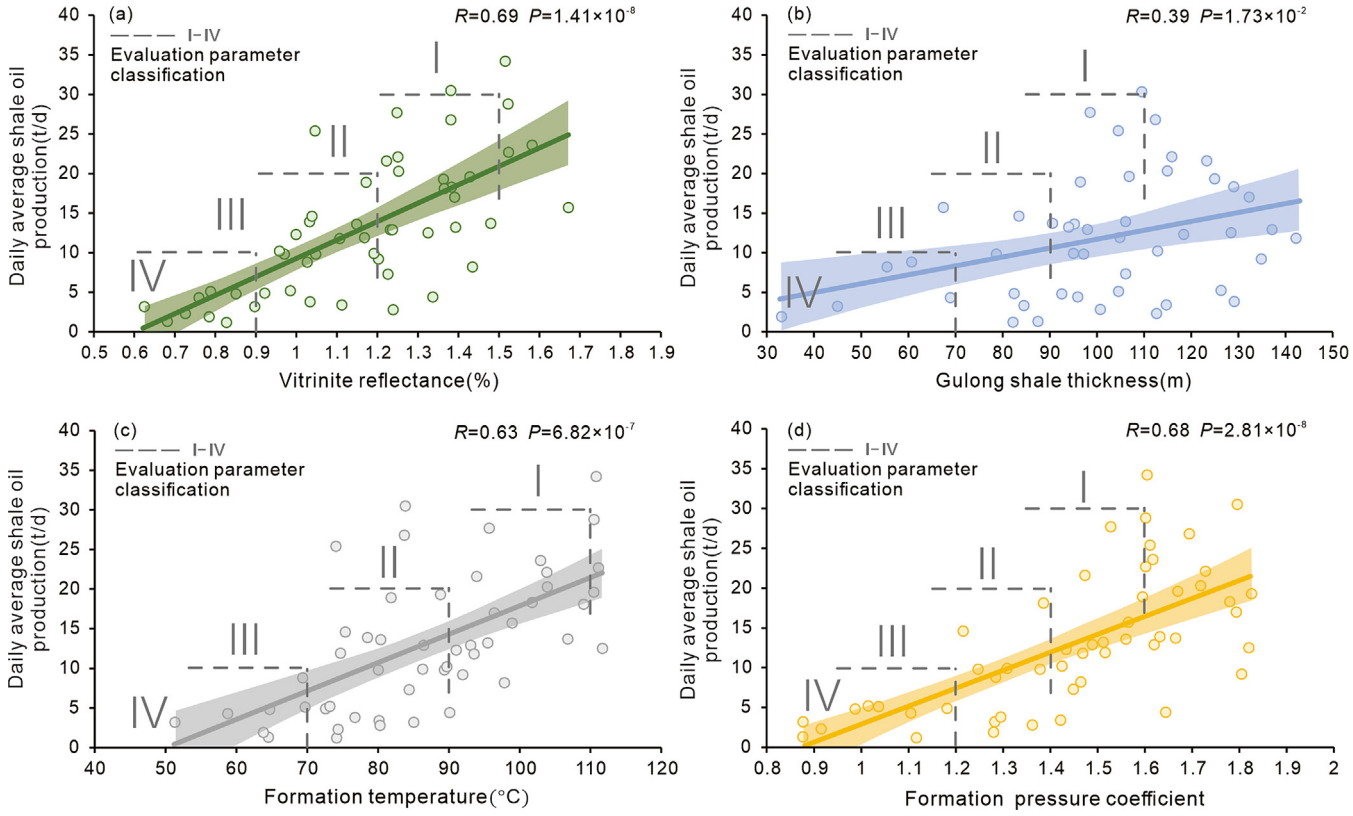

Fig. 12. Intersection plot of optimized evaluation parameters and oil production in the evaluation parameter system.

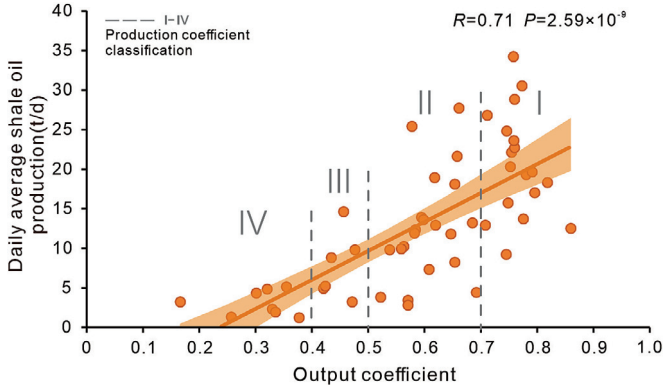

Fig. 13. Relationship between output coefficient (Opc) and oil production capacity.

5. Discussion

5.1. Impact of temperature-pressure coupling on shale oil accumulation

5.1.1. Temperature-pressure conditions promote shale oil generation and enrichment

According to the constructed resource evaluation framework and the results of the Opc-based resource classification, the first-class favorable shale oil zones and high-output regions are predominantly distributed in areas characterized by the coupled conditions of "high temperature + overpressure". To further investigate the controlling mechanism of this coupling on hydrocarbon accumulation, this section selects three representative shale oil wells: Well X10, located in the central Gulong Sag; Well X6, in the marginal area; and Well XY1, in the Sanzhao Sag, for analysis. By examining their burial history, thermal evolution, and pressure evolution processes, the study aims to clarify the role of temperature-pressure evolution in governing shale oil generation and enrichment.

Well X10, located in the central Gulong Sag, has experienced rapid subsidence and continuous deep burial since the deposition of the Mingshui Formation (Fig. 14a). The region was subjected to a strong paleo-heat flow, resulting in a maximum formation temperature of 185 °C, well above the upper limit of the main shale oil generation window (150 °C) (Tang et al., 2024). Between 70 Ma and 40 Ma, the shale interval remained in a sustained high-temperature state, providing favorable conditions for organic matter pyrolysis and secondary cracking. This facilitated the generation of light, high-maturity hydrocarbons with good fluidity (Wan et al., 2024; Wang et al., 2024).

Additionally, Well X10 has been preserved under a sealed overpressure environment for a long time, with a present-day pressure coefficient as high as 1.63. Burial history reveals slow uplift and minor erosion. At the same time, heterogeneities in the Qingshankou Formation's mudstone layers have contributed to the development of overpressure compartment structure, effectively trapping hydrocarbons (Dong et al., 2016; Soeder, 2018; Huang et al., 2024). These dual advantages of "high temperature + high pressure" make this area particularly favorable for shale oil enrichment. Existing studies have shown that elevated temperatures promote the formation of light hydrocarbons, while overpressure suppresses hydrocarbon dissipation and provides essential driving force for production (Dutta, 2002; Zhang et al., 2024).

In contrast to Well X10, the X6 and XY1 well areas display significantly lower shale oil enrichment due to their weaker temperature-pressure field intensity. During their maximum burial stages, the paleo-heat flow in both places was considerably lower than that of the X10 well region (Li, 2015; Tang et al., 2024; Fu

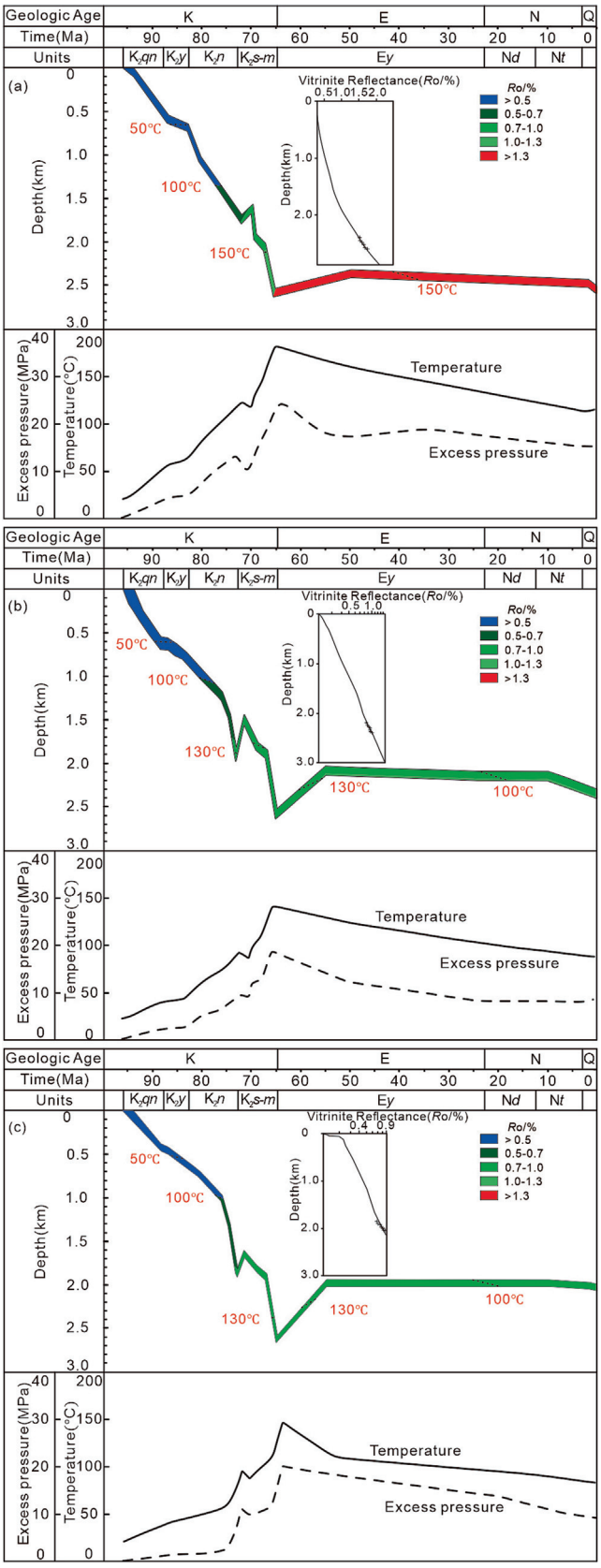

Fig. 14. Temperature and pressure evolution model of the Gulong shale in the central depression: (a) Well X10, (b) Well X6, and (c) Well XY1.

et al., 2025), resulting in only moderate organic matter maturity. In the absence of sufficiently high temperature and pressure, hydrocarbons did not undergo extensive secondary cracking into light components. Moreover, both areas experienced substantial uplift during the late Mingshui Formation, as evidenced by burial history reconstructions (Li, 2015; Shi et al., 2019; Liu et al., 2021), which further reduced present-day thermal and pressure conditions (Fig. 14b and c).

Due to the lack of strong temperature-pressure evolution, the source rocks in Wells X6 and XY1 exhibit limited hydrocarbon generation potential, reduced residual hydrocarbon volumes, and insufficient sealing capacity. These factors collectively lead to moderate or low yield well classifications. The comparison underscores that temperature-pressure field intensity is a key controlling factor in shale oil accumulation, governing both hydrocarbon generation efficiency and reservoir preservation.

In summary, the temperature-pressure evolution histories of the three wells collectively reveal a clear mechanism of evolution together. Elevated temperatures accelerate the thermal evolution of source rocks and promote the generation of light hydrocarbons, while overpressure enhances hydrocarbon retention and significantly increases shale oil productivity. The coupling of high temperature and overpressure thus plays a dominant role in controlling the generation and distribution of shale oil. Moreover, the present-day T-P field configurations effectively reflect the paleo-thermal and pressure evolution trends, offering a reliable geological basis for evaluating shale oil enrichment mechanisms and estimating resource potential.

5.1.2. Present-day temperature and pressure (T-P) fields patterns in identifying shale oil sweet spots

The present-day temperature and pressure (T-P) fields are cumulative manifestations of long-term basin evolution and exhibit distinct spatial distribution patterns that provide direct guidance for delineating shale oil sweet spot zones. Analysis of the temperature and pressure evolution at the three representative wells indicates that since the deposition of the Yian Formation, the Gulong shale interval has experienced a prolonged period of high-temperature and overpressure sealing. This persistent overpressure environment effectively inhibited secondary migration and dissipation of hydrocarbons, thereby enhancing hydrocarbon retention efficiency. The development of such overpressure conditions is primarily driven by rapid subsidence and hydrocarbon generation-induced pressurization (Huang et al., 2024).

Additionally, the present-day T-P field configuration across the basin exhibits strong regional consistency. Among the submembers of the Qingshankou Formation, Member 1 exhibits the highest current geothermal gradient, reaching up to 3.84 °C/km, indicating it has experienced the most intense thermal activity in the basin's geologic history. This strong heat flow regime has promoted rapid organic matter maturation and abundant light oil generation, which are key factors supporting the formation of shale oil sweet spots. Current exploration and development practices have also confirmed that Member 1 is the most productive shale oil interval in the area and holds significant development potential (Cui et al., 2022; Sun et al., 2024).

As shown in Fig. 13, when the formation temperature exceeds 90 °C, the proportion of shale oil wells with daily production greater than 20 t/d increases significantly, and the corresponding Opc values are generally above 0.7. This observation highlights that elevated temperature is a critical factor for high-yield shale oil production. Similarly, zones with pressure coefficients ≥ 1.4 are predominantly associated with high-output wells, reinforcing the dual contribution of overpressure to hydrocarbon retention and enhanced reservoir drive. Based on these findings, this study proposes the criterion of "formation temperature ≥ 90 °C and pressure coefficient ≥ 1.4" as the core standard for identifying shale oil sweet spots in the Gulong shale interval. This temperature-pressure combination not only reflects improved shale oil fluidity

and recoverability but also indicates favorable preservation conditions and sufficient reservoir drive, thereby offering a quantifiable basis for accurately delineating favorable zones.

Furthermore, a review of typical global shale oil basins, such as the Bakken Shale in the Williston Basin and the Wolfcamp Shale in the Permian Basin, reveals that the temperature and pressure conditions of their sweet spots generally fall within the ranges of 80–120 °C and 1.2–1.6, respectively (Cramer, 1992; Tran et al., 2011; Wickard et al., 2016; Khalil et al., 2020; Wu et al., 2021; Li et al., 2023b; Zhou et al., 2023). This suggests that high-temperature and high-pressure regimes serve as universal parameters governing shale oil enrichment in both continental and marine settings (Fig. 15). Such global consistency further confirms that the present-day T-P fields not only reflect the basin's thermal-tectonic evolution but also serve as reliable geological indicators for predicting sweet spots and classifying resources.

5.1.3. Insights into abnormal temperature-pressure conditions

Although the temperature-pressure (T-P) field in the study area generally exhibits a strong coupling evolution trend, localized anomalies in T-P distributions are still observed, which require further interpretation of their genetic mechanisms. Two typical types of abnormal T-P combinations were identified:

(1) High-temperature and low-pressure zones: These are mainly located along the southern margin of the Gulong Sag, such as the area around Well QX1. Preliminary analysis suggests that localized thermal anomalies are induced by hydrothermal activity near fault zones on the hanging wall. Additionally, shale in this region has undergone pressure release due to the development of microfractures, resulting in relatively low formation pressures.

(2) Low-maturity and high-pressure zones: These are primarily distributed in the northern Qijia Sag and the transitional zone between the Daqing Placanticline and surrounding depressions (e.g., Well QX5). In these areas, vitrinite reflectance (R_o) is generally low (<0.8%), yet pressure coefficients exceed 1.3. We interpret this pattern as a result of undercompaction of mudstone caused by early rapid burial, which inhibited normal dewatering and led to overpressure. This interpretation aligns with the explanation proposed by Huang et al. (2024) regarding the genesis of abnormal overpressure in this area.

Notably, an anomalously high vitrinite reflectance (R_o > 1.2%) was observed in the Member 1 interval of Well J6, which contrasts sharply with the relatively low present-day formation temperature of this layer. We infer that this elevated maturity is likely related to episodic hydrothermal disturbances. Deep sourced hydrothermal fluids may have migrated upward along major basement faults, significantly enhancing the local thermal evolution and imprinting a high R_o "thermal signature" on the shale. The occurrence of hydrothermal minerals such as barite within the Member 1 shale may serve as strong mineralogical evidence of such events (He et al., 2022).

In summary, the formation of temperature-pressure anomalies is not solely governed by regional depositional tectonic settings, but may also be significantly affected by late-stage hydrothermal activity and fluid pressure dissipation. Accurate identification and interpretation of these anomalies enhance our understanding of shale oil heterogeneity and accumulation mechanisms, providing valuable supplementary insights for resource evaluation and optimization of exploration strategies.

5.2. Temperature-pressure dominated logic and application in resource evaluation

5.2.1. The role of temperature-pressure fields in resource evaluation systems

In the current field of unconventional hydrocarbon resource evaluation, various methodologies have been developed for predicting and assessing shale oil "sweet spots" including the integrated overlay method, comprehensive index method, weighted factor approach, and well-seismic combined evaluation technique

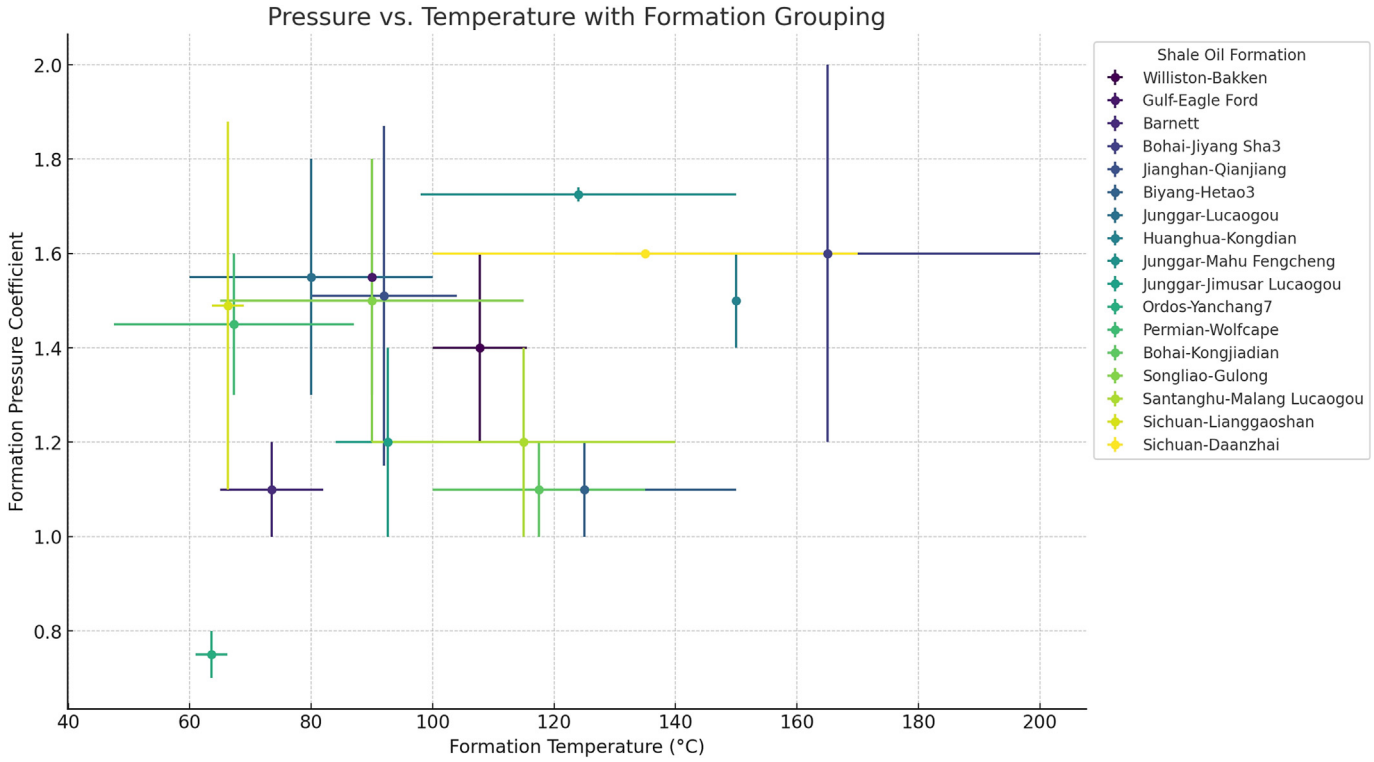

Fig. 15. Distribution of formation pressure and temperature in global shale oil plays.

(Zhou et al., 2020; Li et al., 2022). These approaches are capable of incorporating a wide range of geological and reservoir parameters such as porosity, permeability, organic matter abundance, and effective thickness (Pan et al., 2018; Zhang et al., 2019). However, most of them treat T-P as independent variables, thereby neglecting their synergistic effects in systematically controlling shale oil generation, migration, and preservation processes (Qiu et al., 2018; Sun et al., 2021a).

During geological evolution, the temperature-pressure (T-P) field jointly governs the occurrence state and production potential of shale oil, exerting its control primarily in three aspects. First, under high-temperature and high-pressure conditions, reservoir pore structures tend to be more developed, and fracture systems are more stable and interconnected, which favors the enrichment and preservation of free hydrocarbons and enhances fluid mobility. In contrast, in low-temperature and low-pressure environments, adsorbed hydrocarbons dominate, leading to reduced flow capacity (Johnston, 1987; Li et al., 2023a; Liu et al., 2023a; Zhang and Hou, 2024). Second, elevated formation temperatures reduce the adsorption capacity of organic matter and minerals on hydrocarbons, thus enhancing hydrocarbon mobility, while overpressure inhibits fracture closure and increases formation permeability (Liu et al., 2012; Hsu and Robinson, 2017; Zeng et al., 2023). Third, the T-P combination significantly influences shale oil recoverability: high temperatures reduce oil viscosity and threshold pressure gradient (TPG), whereas overpressure provides additional driving force for production and improves fluid migration efficiency (Wang et al., 2023a; Qu et al., 2024).

Therefore, the coupling of T-P not only governs the processes of shale oil generation and migration, but also plays a dominant role in its preservation and spatial enrichment. The multi-index weighted model developed in this study, based on T-P parameters, leverages the present-day temperature-pressure field as a proxy for paleo-thermal and pressure evolution, and explores its discriminative power in delineating zones of shale oil resource potential. Our results confirm a strong consistency between T-P coupling characteristics and known high-production areas, further substantiating the practical value of T-P fields as a key controlling indicator for identifying shale oil sweet spots.

5.2.2. Construction of a shale oil resource prediction model based on temperature-pressure fields

Incorporating temperature-pressure (T-P) field variables into the traditional comprehensive weighted factor method, this study develops a shale oil resource prediction model that integrates key geological parameters, including vitrinite reflectance (R_o) and effective shale thickness. The variable effective shale thickness reflects the extent of shale layers with favorable hydrocarbon generation potential and reservoir properties; a greater effective shale thickness indicates more substantial resource potential (Lu et al., 2012; Yang et al., 2019; Zhao et al., 2020a). R_o, as a critical indicator of the thermal maturity of source rocks, defines the favorable window for hydrocarbon generation typically between 0.7% and 1.2%, which is considered optimal for shale oil formation (Evenick, 2021; Katz and Lin, 2021).

A notable advantage of the temperature-pressure (T-P) coupling model lies in its ability to simplify the variable framework and mitigate common multicollinearity issues. By clarifying the individual contributions of each parameter to shale oil enrichment, the model enhances scientific rigor, applicability, and practical operability in resource prediction.

The main idea behind this model supports a two-stage "exploration-validation" strategy. In the early exploration phase, the spatial distribution of shale oil sweet spots can be quickly identified using only T-P parameters, offering a preliminary framework for potential resource zones. In the later phase, production data and core-based experimental parameters (e.g., pyrolysis-derived S_1 values) are incorporated to refine and optimize the delineation, enabling higher-precision zoning and evaluation.

Taking the Gulong Sag of the Songliao Basin as a case study, the model constructed based on T-P fields successfully delineated the central sweet spot areas of the Gulong shale during the initial identification phase. When compared with the final delineation refined through the integration of production data and core-derived parameters, the spatial difference in area was only about 24%. At the same time, the dominant distribution zones remained highly consistent (Fig. 16d). This demonstrates that the model possesses strong regional indication capability and interpretability, making it well-suited for rapid deployment and resource evaluation in the early stages of exploration.

5.2.3. Classification standards and resource potential analysis of Gulong shale oil

Based on the temperature-pressure (T-P) dominant control model, this study conducted a classification-based assessment of shale oil resources in the Gulong area of the Songliao Basin. The study area was divided into four favorable zones: Class I areas represent high-temperature and high-pressure enrichment zones with the most significant production potential; Class II areas possess relatively favorable resource conditions and serve as key exploration targets; Class III areas have limited resource potential but still hold localized development value; and Class IV areas exhibit poor geological conditions and low resource potential (Fig. 16). Among them, the areal extents are as follows: Class I – 675 km^2, Class II – 2292 km^2, Class III – 4939 km^2, and Class IV – 21,600 km^2. The estimated shale oil resources for each zone are 710 million tons (Class I), 1.72 billion tons (Class II), 2.47 billion tons (Class III), and 4.32 billion tons (Class IV)(Table A.3), respectively.

A comparison of this study's results with previous assessments based on multi-parameter overlay methods and Monte Carlo simulations reveals a high degree of consistency in both estimated resource volumes and spatial distribution trends (Cui et al., 2020; Zhao et al., 2023; Sun et al., 2024). For instance, Liu et al. (2014) estimated the effective recoverable resources of the Qing 1 Member to be 9.64×10^9 t using the Monte Carlo method; Cui et al. (2020) delineated a sweet spot area of 4200 km^2 with an estimated resource of 3.25×10^9 t; and Wang et al. (2020) calculated the resources of the Qing 1 and Qing 2 Members to be 5.59×10^9 t and 4.43×10^9 t, respectively. The predicted resource volume of Class II areas in this study aligns well with these previous results, indicating that the temperature-pressure model exhibits strong consistency and adaptability in total resource estimation.

It is worth noting that although the estimated resource volume of Class I areas in this study appears relatively low, this does not indicate an underestimation. Instead, it reflects the model's emphasis on the three key elements of "high-quality preservation, efficient migration, and effective retention." The temperature and pressure (T-P) dominated model selectively identifies areas with advanced thermal maturity, strong pressure sealing capacity, and stable production potential, thereby enhancing the precision and targeting of resource evaluation. In contrast to traditional multi-parameter overlay methods that may overestimate the extent of enrichment zones, the T-P dominant model more accurately captures the mechanisms of free hydrocarbon preservation and the integrity of fluid migration barriers.

5.2.4. Validation of method reliability and future applications

To validate the effectiveness of the temperature-pressure (T-P) coupling-based resource evaluation model proposed in this study,

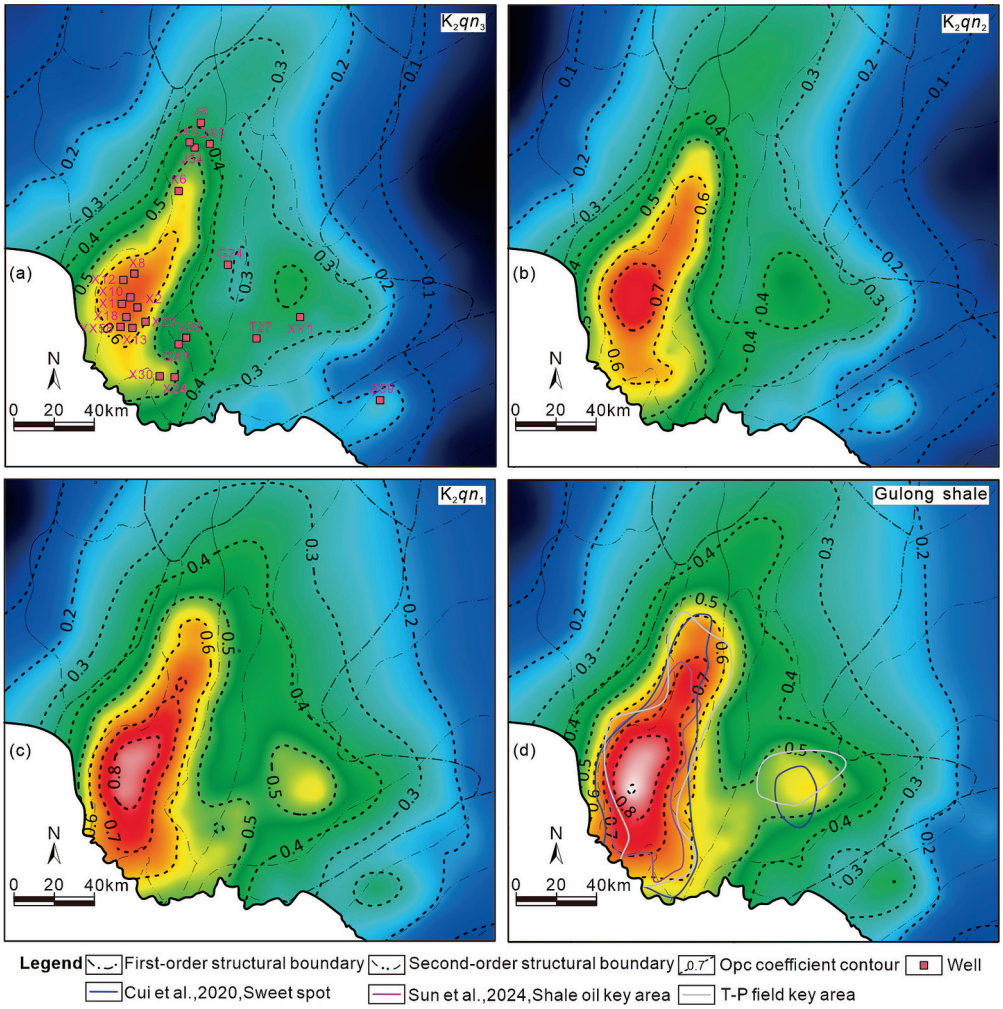

Fig. 16. Maps of favorable zones in the Qingshankou shale oil reservoir, Central Depression. Contour maps of the Opc coefficient are shown for (a) Member 3, (b) Member 2, (c) Member 1 of the Qingshankou Formation, and (d) the Gulong Shale. The blue and purple circled areas indicate favorable zones identified through various assessment methods (refer to Cui et al., 2020; Sun et al., 2024).

we conducted systematic comparisons and verification at both regional and well scales. At the regional scale, the sweet spot areas delineated by this model show high consistency with previous results obtained using multi-parameter overlay and volumetric methods (Sun et al., 2023a, 2024). The greatest alignment is observed in the central Gulong Sag, indicating that T-P parameters play a key role in controlling shale oil resource evaluation.

At the well scale, the model's evaluation results demonstrate strong consistency with actual production performance. For example, Wells X18, X13, and X24 all exhibit formation temperatures exceeding 105 °C and pressure coefficients greater than 1.55. Their corresponding daily oil productions reach 27 t/d, 32 t/d, and 25 t/d, respectively, with Opc indices all exceeding 0.79, placing them firmly within Class I favorable zones. This high level of agreement underscores the practical utility of the temperature-pressure-dominated model in accurately predicting high-production enrichment areas.

It is worth noting that the model exhibits certain limitations in applicability when locally evaluating the previously identified anomalous zones, specifically those characterized by high temperatures and low pressures, as well as those described by low temperatures and high pressures. Although the model remains instructive for large-scale delineation, the resource distribution and preservation conditions in these anomalous areas require additional geological background constraints and supplementary interpretation. Future research should focus on refining the model's adaptability in these contexts.

Furthermore, this method shows strong potential for regional transferability. Given its validated performance in the Gulong Sag of the Songliao Basin, the model could potentially be applied to other continental shale basins with similar thermal regimes and abnormal pressure structures, such as the Ordos Basin and the Sichuan Basin, as well as international counterparts like the Bakken and Vaca Muerta formations.

In future developments, we plan to incorporate machine learning techniques such as XGBoost to model the nonlinear relationships among T-P parameters, vitrinite reflectance (R_o), pyrolysis parameter S_1, and recoverable oil production. This approach aims to enhance the model's predictive capabilities. Furthermore, by integrating interpretable algorithms such as SHAP values and decision trees, we can alleviate the "black-box" nature of traditional models, enabling geological traceability of variable weights and evaluation logic. Although challenges like data dependency and physical constraints remain, the T-P based evaluation method shows a clear structure and strong adaptability, offering a solid foundation for rapid prediction and zonation of unconventional shale oil resources.

6. Summary and conclusions

Using the Qingshankou Formation in the central depression zone of the Songliao Basin as a case study, this research systematically analyzed the current temperature-pressure (T-P) field distribution. It developed a multi-factor model for evaluating shale oil resources. The study performed shale oil resource classification and identified favorable zones, clarified the main geological factors controlling shale oil accumulation, and discussed the applicability of the proposed method. The main conclusions are as follows.

(1) The areas with high T-P formation in the Qingshankou Formation are mainly found in the central and southern parts of the Qijia-Gulong Sag. Formation temperatures mostly exceed 75 °C, reaching up to 121 °C, and pressure coefficients are generally above 1.4. These elevated temperature and overpressure conditions improve hydrocarbon mobility and retention, creating favorable geological conditions for shale oil accumulation.

(2) The resource evaluation model incorporating temperature-pressure (T-P) fields successfully delineates four categories of shale oil enrichment zones. Class I and II zones, identified as the most favorable for development, are primarily distributed in the central and southern Gulong Sag, as well as the southwestern part of the Sanzhao Sag, with estimated resources of 710 million tonnes and 1.72 billion tonnes, respectively. The study highlights that in lacustrine shale at the same stratigraphic level, prioritizing high-temperature and high-pressure regions as sweet spot candidates is a key principle for resource evaluation. For instance, in the Gulong shale oil system, a formation temperature of $\geq$ 90 °C and a pressure coefficient of $\geq$ 1.4 can serve as critical thresholds for identifying sweet spots, providing clear engineering guidance.

(3) The combined effects of formation T-P mainly control the creation and enrichment of shale oil. Higher temperatures speed up the thermal maturation of source rocks and increase the production of light hydrocarbons, which improves hydrocarbon fluidity. At the same time, overpressure enhances the sealing capacity for free hydrocarbons, preventing their escape and supporting the buildup of high-quality shale oil. The interaction between these two factors not only influences the occurrence state of shale oil but also impacts its development potential. The current temperature-pressure distribution serves as a useful indicator of historical thermal and pressure changes, providing a solid geological basis for identifying shale oil-rich zones and assessing resource prospects.

(4) The proposed evaluation method shows strong applicability and potential for wider adoption. Besides the Songliao Basin, the temperature-pressure dominated model can be applied to other continental shale basins with high heat flow and overpressure conditions, such as the Ordos Basin, Sichuan Basin, and North America's Bakken and Vaca Muerta formations.

CRediT authorship contribution statement

Yue Huang: Conceptualization, Data curation, Formal analysis, Investigation, Methodology, Software, Validation, Visualization, Writing – original draft, Writing – review & editing. **Jian Chang:** Conceptualization, Data curation, Funding acquisition, Project administration, Resources, Supervision, Validation, Writing – original draft, Writing – review & editing. **Nansheng Qiu:** Conceptualization, Funding acquisition, Project administration, Resources, Supervision, Writing – original draft, Writing – review & editing. **Nobuo Maeda:** Supervision, Writing – original draft, Writing – review & editing.

Declaration of Competing Interest

The authors declare that they have no known competing financial interests or personal relationships that could have appeared to influence the work reported in this paper.

Acknowledgements

This study was primarily supported by the National Key Research and Development Program (Grant No. 2021YFA0716003). Comments from the anonymous reviewers were helpful in improving the manuscript.

Appendix A. Supplementary data

Table A.1
Evaluation criteria for favorable production classification of Gulong shale oil reservoirs.

Gulong shale thickness (m)	Formation pressure coefficient (P_c)	Vitrinite reflectance (R_o)	Formation temperature T (°C)	Grading
< 70	$P_c \leq 1.2$	$R_o < 0.9$	< 70	IV
70–90	$1.2 < P_c \leq 1.4$	$0.9 < R_o < 1.2$	70–90	III
90–110	$1.4 < P_c \leq 1.6$	$1.2 < R_o < 1.5$	90–110	II
110 <	$1.6 < P_c$	$1.5 < R_o$	110 <	I

Table A.2
Evaluation criteria for production coefficient classification.

Q_{pc} Value	0.3 – 0.4	0.4 – 0.5	0.5 – 0.7	0.7 – 0.9
Classification	IV	III	II	I

Table A.3
Evaluation results of shale oil resources in pure shale sections of the Qingshankou Formation, Songliao Basin.

Stratum	Type I geological resources/10%	Type II geological resources/10%	Type III geological resources/10%	Type IV geological resources/10%
Gulong Shale	7.1	17.2	24.7	43.2
Qing 1 Member	5.3	13.5	16.8	27.6
Qing 2 Member	2.8	7.9	11.1	13.6
Qing 3 Member	1.4	4.2	6.3	7.9

References

Akkutlu, I.Y., Baek, S., Olorode, O.M., Wei, P., Tongyi, Z., Shuang, A., 2017. Shale resource assessment in presence of nanopore confinement. SPE/AAPG/SEG Unconventional Resources Technology Conference, URTEC,, 70–80.

Bai, X., Chen, R.Q., Shang, F., Zhang, N., 2024. Sedimentary environment and oil-bearing characteristics of shale in Cretaceous Qingshankou Formation in Songliao Basin. Petrol. Geol. Exp. 46 (5), 1063–1074 (in Chinese with English abstract).

Bullard, E.C., 1939. Heat flow in South Africa. Proc. R. Soc. Lond. A Math. Phys. Sci. 173, 474–502.

Cao, D., Zeng, L., Gomez-Rivas, E., Gong, L., Liu, G., Lu, G., Bons, P.D., 2024. Correction of linear fracture density and error analysis using underground borehole data. J. Struct. Geol. 184, 105–152.

Chen, B., Pan, S., Fang, L., Zhang, Q., Li, C., Liang, S., 2016. Reservoir characteristics of mudstone (shale) interval in the Qingshankou Formation, Qijia-Gulong Sag, Songliao Basin, Northeast China. Nat. Gas Geosci. 27 (2), 298–308.

Chen, Y., 1996. Study and evaluation of oil source rock using log data. Geophysical Prospecting for Petroleum 35 (1), 99–106 (in Chinese with English).

Chen, Z., Li, M., Jiang, C., Qian, M., 2019. Shale oil resource potential and its mobility assessment: A case study of Upper Devonian Duvernay shale in western Canada sedimentary basin. Oil Gas Geol. 40, 459–468 (in Chinese with English abstract).

Cramer, D.D., 1992. Treating-pressure analysis in the Bakken Formation. J. Petrol. Technol. 44, 20–27.

Cui, B., Chen, C., Lin, X., Zhao, Y., Cheng, X., Zhang, Y., Lu, G., 2020. Characteristics and distribution of sweet spots in Gulong shale oil reservoirs of Songliao Basin. Pet. Geol. Oilfield Dev. Daqing 39, 45–55 (in Chinese with English abstract).

Cui, B., Wang, R., Bai, Y., Liu, L., Liu, X., Wang, J., Liu, Z., 2024. Exploration and development progress and development strategies of Gulong shale oil. Pet. Geol. Oilfield Dev. Daqing 43, 125–136 (in Chinese with English abstract).

Cui, B., Zhao, Y., Zhang, G., Sun, X., Zhang, Y., Bai, Y., Zhang, Y., 2022. Estimation method and application for OOIP of Gulong shale oil in Songliao Basin. Pet. Geol. Oilfield Dev. Daqing 41, 14–23 (in Chinese with English abstract).

Dong, D., Zou, C., Dai, J., Huang, S., Zheng, J., Gong, J., Wang, Y., Li, X., Guan, Q., Zhang, C., Huang, J., Wang, S., Liu, D., Qiu, Z., 2016. Suggestions on the development strategy of shale gas in China. J. Nat. Gas Geosci. 1 (6), 413–423.

Dutta, N.C., 2002. Deepwater geohazard prediction using prestack inversion of large offset p-wave data and rock model. Lead. Edge 21, 193–198.

Zou, C., Dong, D., Wang, Y., Li, X., Huang, J., Wang, S., Guan, Q., Zhang, C., Wang, H., Liu, H., Bai, W., Liang, F., Lin, W., Zhao, Q., Liu, D., Yang, Z., Liang, P., Sun, S., Qiu, Z., 2016. Shale gas in China: Characteristics, challenges and prospects (II). Petrol. Explor. Dev. 43 (2), 182–196.

Eaton, B.A., 1975. The equation for geopressure prediction from well logs, in: SPE Annual Technical Conference and Exhibition, SPE, pp. SPE–5544–MS.

Evenick, J.C., 2021. Examining the relationship between tmax and vitrinite reflectance: An empirical comparison between thermal maturity indicators. J. Nat. Gas Sci. Eng. 91, 103946.

Fu, X., Chang, J., Tang, B., Zhu, C., Li, X., Huang, Y., Su, Y., Xu, Q., Meng, Q., 2025. Rapid maturation evolution of the shale oil in the heat sedimentary basins: A case study of the Qijiagulong Sag in Songliao Basin, northeastern China. Chin. J. Geophys. 68, 182–198 (in Chinese with English abstract).

Guo, Q., Wu, J., Chen, X., Chen, N.S., Wu, X.Z., Liu, Z.X.X., 2021. Discussion on evaluation method of total oil and movable oil in-place. Oil Gas Geol. 42, 1451–1463 (in Chinese with English abstract).

Hao, J., Zhou, C., Li, X., Cheng, X., Li, C., Song, L., 2012. Summary of shale gas evaluation applying geophysical logging. Prog. Geophys. 27 (4), 1624–1632 (in Chinese with English abstract).

He, W., Meng, Q., Feng, Z., Zhang, J., Wang, R., 2022. In-situ accumulation theory and exploration & development practice of Gulong shale oil in Songliao Basin. Acta Pet. Sin. 43 (1), 1–14 (in Chinese with English abstract).

He, W.Y., Meng, Q.A., Zhang, J.Y., 2021. Controlling factors and their classification-evaluation of Gulong shale oil enrichment in Songliao Basin. Pet. Geol. Oilfield Dev. Daqing 40, 1–12 (in Chinese with English abstract).

Hsu, C.S., Robinson, P.R., 2017. Springer Handbook of Petroleum Technology. Springer.

Hu, S., Bai, B., Tao, S., Bian, C., Zhang, T., Chen, Y., Liang, X., Wang, L., Zhu, R., Jia, J., Pan, Z., Li, S., Liu, Y., 2022. Heterogeneous geological conditions and differential enrichment of medium and high maturity continental shale oil in China. Petrol. Explor. Dev. 49, 257–271.

Hu, T., Pang, X., Jiang, F., Wang, Q., Liu, X., Wang, Z., Jiang, S., Wu, G., Li, C., Xu, T., 2021. Movable oil content evaluation of lacustrine organic-rich shales: Methods and a novel quantitative evaluation model. Earth-Sci. Rev. 214, 103545.

Huang, Y., Chang, J., Qiu, N., Lin, T., Fu, X., Tang, B., Li, J., 2024. Pressure field characteristics and overpressure geneses of Qingshankou Formation in Qijia-Gulong sag, Songliao Basin. Acta Pet. Sin. 45 (12), 1800–1817 (in Chinese with English abstract).

Jarvie, D.M., 2012. Shale resource systems for oil and gas: Part 2-shale-oil resource systems. AAPG Mem.

Jia, C., Pang, X., 2015. Research processes and main development directions of deep hydrocarbon geological theories. Acta Pet. Sin. 36 (12), 1457–1469 (in Chinese with English abstract).

Johnston, D.H., 1987. Physical properties of shale at temperature and pressure. Geophysics 52, 1391–1401.

Kang, S., Yang, Y., Wang, H., Jiang, W., He, K., Liu, R., 2023. Oil-bearing capacity of shale in the first member of upper Cretaceous Qingshankou Formation, Sanzhao Sag, Central Depression, Songliao Basin. Petrol. Geol. Exp. 45, 89–98 (in Chinese with English abstract).

Katz, B.J., Lin, F., 2021. Consideration of the limitations of thermal maturity with respect to vitrinite reflectance, tmax, and other proxies. AAPG Bull. 105, 695–720.

Khalil, R., Ramezanian, M., Altawati, F., Emadi, H., 2020. Evaluating pressure and temperature effects on permeability and elastic properties of Wolfcamp Formation–an experimental study, in: ARMA US Rock Mechanics/Geomechanics Symposium, ARMA, pp. ARMA–2020.

Li, J., Jiang, C., Wang, M., Lu, S., Chen, Z., Chen, G., Li, J., Li, Z., Lu, S., 2020. Adsorbed and free hydrocarbons in unconventional shale reservoir: A new insight from NMR T_1–T_2 maps. Mar. Pet. Geol. 116, 104311.

Li, J., Wang, M., Lu, S., Liu, L., Li, M., Zhang, Y., Wang, X., Zhao, X., Zhang, J., Zhao, Y., 2023a. Quantitative evaluation model of shale oil adsorption: a case study of the first member of Cretaceous Qingshankou Formation in northern Songliao Basin, NE China. Petrol. Explor. Dev. 50, 1137–1150.

Li, J., Yang, Z., Wang, Z., Tang, Y., Zhang, H., Jiang, W., Wang, X., Wei, Q., 2023b. Quantitative characterization and main controlling factors of shale oil occurrence in Permian Fengcheng Formation, Mahu Sag, Junggar Basin. Petrol. Geol. Exp. 45, 681–692 (in Chinese with English abstract).

Li, S., Zhang, J., Gong, F., Zhu, H., Bai, Y., 2017. The characteristics of mudstones of upper Cretaceous Qingshankou Formation and favorable area optimization of shale oil in the north of Songliao Basin. Geol. Bull. China 36, 654–663 (in Chinese with English abstract).

Li, X.W., 2015. Numerical simulations of the burial & thermal histories for Daqing placanticline in north Songliao Basin. Pet. Geol. Oilfield Dev. Daqing 34, 46–50 (in Chinese with English abstract).

Li, Y., Zhao, Q., Lyu, Q., Xue, Z., Cao, X., Liu, Z., 2022. Evaluation technology and practice of continental shale oil development in China. Petrol. Explor. Dev. 49, 1098–1109.

Lin, W., Gan, H., Zhao, Z., Zhang, S., 2023. Lithospheric thermal-rheological structure and geothermal significance in the Gonghe Basin, Qinghai Province. Acta Geosci. Sin. 44, 45–56 (in Chinese with English abstract).

Liu, B., He, J., Lv, Y., Ran, Q., Dai, C., Li, M., 2014. Parameters and method for shale oil assessment: Taking Qinshankou Formation shale oil of northern Songliao Basin. J. Cent. South Univ. 45, 3846–3852 (in Chinese with English abstract).

Liu, B., Lü, Y., Zhao, R., Tu, X., Guo, X., Shen, Y., 2012. Formation overpressure and shale oil enrichment in the shale system of Lucaogou Formation, Malang Sag, Santanghu Basin, NW China. Petrol. Explor. Dev. 39, 744–750.

Liu, B., Mohammadi, M.R., Ma, Z., Bai, L., Wang, L., Xu, Y., Hemmati-Sarapardeh, A., Ostadhassan, M., 2023a. Pore structure evolution of Qingshankou shale (kerogen type I) during artificial maturation via hydrous and anhydrous pyrolysis: Experimental study and intelligent modeling. Energy 282, 128359.

Liu, B., Shi, J., Fu, X., Lyu, Y., Sun, X., Gong, L., Bai, Y., 2018. Petrological characteristics and shale oil enrichment of lacustrine fine-grained sedimentary system: A case study of organic-rich shale in first member of Cretaceous Qingshankou Formation in Gulong Sag, Songliao Basin, NE China. Petrol. Explor. Dev. 45, 884–894.

Liu, B., Sun, J., Zhang, Y., He, J., Fu, X., Yang, L., Xing, J., Zhao, X., 2021. Reservoir space and enrichment model of shale oil in the first member of Cretaceous Qingshankou Formation in the Changling Sag, southern Songliao Basin, NE China. Petrol. Explor. Dev. 48, 608–624.

Liu, B., Wang, H., Fu, X., Bai, Y., Bai, L., Jia, M., He, B., 2019. Lithofacies and depositional setting of a highly prospective lacustrine shale oil succession from the upper Cretaceous Qingshankou Formation in the Gulong Sag, northern Songliao Basin, Northeast China. AAPG Bull. 103, 405–432.

Liu, B., Wang, L., Fu, X., Huo, Q., Bai, L., Lv, J., Wang, B., 2023b. Identification, evolution and geological indications of solid bitumen in shales: A case study of the first member of Cretaceous Qingshankou Formation in Songliao Basin, NE China. Petrol. Explor. Dev. 50, 1345–1357.

Lu, J., Lin, T., Li, J., 2024. Coupling mechanism of Gulong shale oil enrichment in Songliao Basin. Pet. Geol. Oilfield Dev. Daqing 43, 62–74 (in Chinese with English abstract).

Lu, S., Huang, W., Chen, F., Li, J., Wang, M., Xue, H., Wang, W., Cai, X., 2012. Classification and evaluation criteria of shale oil and gas resources: Discussion and application. Petrol. Explor. Dev. 39, 268–276.

Lu, S., Xue, H., Wang, M., Xiao, D., Huang, W., Li, J., Xie, L., Tian, S., Wang, S., Li, J., 2016. Several key issues and research trends in evaluation of shale oil. Acta Pet. Sin. 37 (10), 1309–1322 (in Chinese with English abstract).

Ma, X., Zhu, C., Lin, Y., Shu, Y., 2017. Evolution of the temperature-pressure system and far-source hydrocarbon accumulation in Junggar Basin. Petrol. Geol. Exp. 39, 467–476 (in Chinese with English abstract).

McGlade, C., 2012. A review of the uncertainties in estimates of global oil resources. Energy 47, 262–270.

Meng, Q., Zhang, J.Y., Wu, W., Kang, D.J., Wang, J.W., Yu, D., Sun, Z.Y., Liu, L.J., Liu, S., Liu, J.F., Zhang, Z.C., Yu, T.T., 2024. Geological conditions and exploration potential of interbedded shale oil in Qingshankou Formation of northern Songliao Basin. Pet. Geol. Oilfield Dev. Daqing 43 (3), 38–48 (in Chinese with English abstract).

Meng, Q., Lin, T.F., Zhang, J.Y., Liu, Z., Lv, J.C., Cheng, X.Y., 2022. In-situ accumulation process and reservoir characteristics of shale oil: A case study of Gulong shale oil in Songliao Basin. Pet. Geol. Oilfield Dev. Daqing 41(3), 24-37 (in Chinese with English abstract).

Niu, D.M., Li, Y.L., Zhang, Y.F., Sun, P.C., Wu, H.G., Fu, H., Wang, Z.Q., 2022. Multi-scale classification and evaluation of shale reservoirs and 'sweet spot'

prediction of the second and third members of the Qingshankou Formation in the Songliao Basin based on machine learning. J. Petrol. Sci. Eng. 216, 110678.
Pan, R., Chen, M., Zhang, C., Pan, J., 2018. Seismic prediction of paleogene shale oil "sweet spots" and its influencing factor analysis in the Bonan sub-sag, Jiyang depression. Earth Sci. Front. 25 (4), 142-154 (in Chinese with English abstract).
Qiu, N., Liu, W., Xu, Q., Liu, Y., Chang, J., 2018. Temperature-pressure field and hydrocarbon accumulation in deep-ancient marine strata. Earth Sci. 43, 3511–3525 (in Chinese with English abstract).
Qu, J., Tang, Z., Lei, G., Wu, Q., Liao, Q., Ning, F., 2024. A novel threshold pressure gradient model and its influence on production simulation for shale oil reservoirs. Energy Fuels 38, 11644–11661.
Ren, Z., Qi, K., Yang, G., Cui, J., Yang, P., Wang, K., 2020. Research status and existing problems of relationship between deep thermal evolution history and oil and gas in sedimentary basins. Unconv. Oil Gas 7 (3), 1–7 (in Chinese with English abstract).
Shi, L., Qi, Y., Zhang, Y., Wang, Z., Wang, B., 2019. Numerical simulation of geohistory of the Qijia area in the Songliao Basin and geological significance. Geol. Explor. 55 (2), 661–672 (in Chinese with English abstract).
Soeder, D.J., 2018. The successful development of gas and oil resources from shales in North America. J. Petrol. Sci. Eng. 163, 399–420.
Sorrell, S., Speirs, J., Bentley, R., Brandt, A., Miller, R., 2010. Global oil depletion: A review of the evidence. Energy Policy 38, 5290–5295.
Sun, L., Liu, H., He, W., Li, G., Zhang, S., Zhu, R., Jin, X., Meng, S., Jiang, H., 2021b. An analysis of major scientific problems and research paths of Gulong shale oil in Daqing Oilfield, NE China. Petrol. Explor. Dev. 48, 527–540.
Sun, C., Nie, H., Dang, W., Chen, Q., Zhang, G., Li, W., Lu, Z., 2021a. Shale gas exploration and development in China: Current status, geological challenges, and future directions. Energy Fuels 35, 6359–6379.
Sun, L., Cui, B., Zhu, R., Wang, R., Feng, Z., Li, B., Zhang, J., Gao, B., Wang, Q., Zeng, H., Liao, Y., Jiang, H., 2023a. Shale oil enrichment evaluation and production law in Gulong Sag, Songliao Basin. NE China. Petrol. Explor. Dev. 50 (3), 505–519.
Sun, L., Fang, C., Li, F., Zhu, R., Zhang, Y., Yuan, X., Jia, A., Gao, X., Su, L., 2015. Innovations and challenges of sedimentology in oil and gas exploration and development. Petrol. Explor. Dev. 42, 143–151.
Sun, L., He, W., Feng, Z., Zeng, H., Jiang, H., Pan, Z., 2022. Shale oil and gas generation process and pore fracture system evolution mechanisms of the continental Gulong shale, Songliao Basin, China. Energy Fuels 36, 6893–6905.
Sun, L., Jia, C., Zhang, J., Cui, B., Bai, J., Huo, Q., Xu, X., Liu, W., Zeng, H., Liu, W., 2024. Resource potential of Gulong shale oil in the key areas of Songliao Basin. Acta Pet. Sin. 45 (12), 1699–1714 (in Chinese with English abstract).
Sun, L., Zhao, W., Liu, H., Zhu, R., Bai, B., Kang, Y., Zhang, J., Wu, S., 2023b. Concept and application of "sweet spot" in shale oil. Acta Pet. Sin. 44, 1.
Tan, J., Wu, K., Li, Y., Zhao, X., Yan, C., Huang, Z., Du, Z., Li, S., 2021. Application of logging prediction toc method in shale reservoir evaluation. Prog. Geophys. 36 (1), 258–266 (in Chinese with English abstract).
Tang, B., Qiu, N., Zhu, C., Chang, J., Li, X., Huang, Y., Yang, J., Fu, X., 2024. Thermal conductivity column of rocks and distribution characteristics of paleo-geothermal field in the Songliao Basin. Coal Geol. Explor. 52 (1), 26–35 (in Chinese with English abstract).
Tran, T., Sinurat, P., Wattenbarger, R., 2011. Production characteristics of the bakken shale oil. In: SPE Annual Technical Conference and Exhibition? SPE, pp. SPE–145684.
Wan, T., Chen, S., Wu, X., Chen, G., Zhang, X., 2024. An investigation on the pyrolysis of low-maturity organic shale by different high temperature fluids heating. Fuel 374, 132498.
Wang, F., Feng, Z., Wang, X., Zeng, H., 2023a. Effect of organic matter, thermal maturity and clay minerals on pore formation and evolution in the Gulong Shale, Songliao Basin. China. Geoenergy Sci. Eng. 223, 211507.
Wang, F., Fu, Z., Wang, J., 2021. Characteristics and classification evaluation of Gulong shale oil reservoir in Songliao Basin. Pet. Geol. Oilfield Dev. Daqing 40, 144–156 (in Chinese with English abstract).
Wang, L., Zeng, W., Xia, X., Zhou, H., Bi, H., Shang, F., Zhou, X., 2019a. Study on lithofacies types and sedimentary environment of black shale of Qingshankou Formation in Qijia-Gulong Depression. Songliao Basin. Nat. Gas Geosci. 30, 1125–1133.
Wang, M., Guo, Z., Jiao, C., Lu, S., Li, J., Xue, H., Li, J., Li, J., Chen, G., 2019b. Exploration progress and geochemical features of lacustrine shale oils in China. J. Petrol. Sci. Eng. 178, 975–986.
Wang, Q., Hao, F., Zhou, S., Xue, Y., Zou, H., Liu, J., 2024. Oil cracking under closed-system pyrolysis: Implications for deep oil occurrence and related source determination. Mar. Pet. Geol. 166, 106928.
Wang, S., 2018. Shale gas exploitation: Status, problems and prospect. Nat. Gas Ind. B 5 (1), 60–74.
Wang, S., Nie, H., Ma, S., Ding, Y., Li, H., Liang, W., 2022. Resource evaluation and sweet-spot prediction of inter-salt shale oil of Paleogene Qianjiang Formation, Qianjiang Sag, Jianghan Basin. Petrol. Geol. Exp. 44, 94–101 (in Chinese with English abstract).
Wang, X., Chen, J., Ren, D., 2023b. Research progress and prospect of pore structure representation and seepage law of continental shale oil reservoir. Petrol. Reserv. Eval. Dev. 13 (1), 23–30 (in Chinese with English abstract).
Wang, Y., Liang, J., Zhang, J., Zhao, B., Zhao, Y., Liu, X., Xia, D., 2020. Resource potential and exploration direction of Gulong shale oil in Songliao Basin. Pet. Geol. Oilfield Dev. Daqing 39, 20–34 (in Chinese with English abstract).
Wei, Y., Li, J., Lu, S., Song, Z., Zhao, R., Zhang, Y., Wang, J., Liu, X., 2021. Comprehensive evaluation method of sweet spot zone in lacustrine shale oil reservoir and its application: A case study of shale oil in lower 1st member of the Shahejie Formation in the Raoyang Sag. J. China Univ. Min. Technol. 50 (5), 813–824 (in Chinese with English abstract).
Wickard, A.K., Elmore, R.D., Heij, G., 2016. A diagenetic study of the Wolfcamp shale, Midland Basin, west Texas, in: SPE/AAPG/SEG Unconventional Resources Technology Conference, URTEC, pp. URTEC–2460784.
Wu, C., Xu, C., Chen, Y., Tan, Q., Xu, T., 2021. The horizontal well exploitation practice of Jimsar shale oil. J. Southwest Pet. Univ. (Sci. Technol. Ed.) 43, 33–41 (in Chinese with English abstract).
Xin, F., Jiang, Y., Liu, J., Sun, B., Jing, C., 2019. Relationship between geothermal-geopressure system and hydrocarbon distribution in north part of dongpu depression. J. Petrochem. Univ. 32, 51.
Xu, Y., Lun, Z., Pan, Z., Wang, H., Zhou, X., Zhao, C., Zhang, D., 2022. Occurrence space and state of shale oil: A review. J. Petrol. Sci. Eng. 211, 110183.
Yang, Z., Hou, L., Tao, S., Cui, J., Wu, S., Lin, S., Pan, S., 2015. Formation conditions and "sweet spot" evaluation of tight oil and shale oil. Petrol. Explor. Dev. 42, 555–565 (in Chinese with English abstract).
Yang, Z., Zou, C.N., Wu, S.T., Lin, S.H., Pan, S.Q., Niu, X.B., Men, G.T., Tang, Z.X., Li, G.H., Zhao, J.D., Jia, X.Y., 2019. Formation, distribution and resource potential of the "sweet areas (sections)" of continental shale oil in China. Mar. Pet. Geol. 102, 48–60.
Yuan, S., Lei, Z., Li, J., Yao, Z., Li, B., Wang, R., Liu, Y., Wang, Q., 2023. Key theoretical and technical issues and countermeasures for effective development of Gulong shale oil, Daqing Oilfield, NE China. Petrol. Explor. Dev. 50 (3), 638–650.
Zeng, L., Gong, L., Zhang, Y., Dong, S., Lyu, W., 2023. A review of the genesis, evolution, and prediction of natural fractures in deep tight sandstones of China. AAPG Bull. 107, 1687–1721.
Zhang, J., 2021. Evaluation of favorable areas of shale oil based on principal component analysis: Taking Daanzhai member of Yilong-Pingchang area as an example. Fault-Block Oil Gas Field 28 (1), 28–32 (in Chinese with English abstract).
Zhang, L., Bao, Y., Li, J., Li, Z., Zhu, R., Zhang, J., 2014. Movability of lacustrine shale oil: a case study of Dongying Sag, Jiyang Depression, Bohai Bay Basin. Petrol. Explor. Dev. 41 (6), 703–711.
Zhang, P., Lu, S., Li, J., Xue, H., Li, W., Zhang, Y., Wang, S., Feng, W., 2019. Identification method of sweet spot zone in lacustrine shale oil reservoir and its application: A case study of the Shahejie Formation in Dongying Sag, Bohai Bay Basin. Oil Gas Geol. 40, 1339–1350 (in Chinese with English abstract).
Zhang, Q., Hou, G., 2024. Research progress on the evaluation of shale oil mobility: Geological characteristics and integrated assessment methods. Adv. Resour. Res. 4 (4), 551–581.
Zhang, X., Cao, Z., Zhou, F., Chen, Y., Ju, P., Yang, X., Xia, Y., Zhang, X., 2022. Hydrocarbon yield evolution characteristics and geological significance in temperature-pressure controlled simulation experiment. J. Nat. Gas Geosci. 7 (6), 385–400.
Zhang, X., Lu, Y., Jin, Y., Chen, M., Zhou, B., 2024. An adaptive physics-informed deep learning method for pore pressure prediction using seismic data. Petrol. Sci. 21, 885–902.
Zhao, W., Bian, C., Li, Y., Liu, W., Qin, B., Pu, X., Jiang, J., Liu, S., Guan, M., Dong, J., Shen, Y., 2024. "Component flow" conditions and its effects on enhancing production of continental medium-to-high maturity shale oil. Petrol. Explor. Dev. 51 (4), 826–838.
Zhao, W., Wang, Z., Huang, F., Zhao, Z., Jiang, H., Xu, Y., 2023. Hydrocarbon accumulation conditions and exploration position of ultra-deep reservoirs in onshore superimposed basins of China. Acta Pet. Sin. 44 (12), 2020-2032 (in Chinese with English abstract).
Zhao, X., Zhou, L., Pu, X., Shi, Z., Han, G., Wu, J., Han, W., Zhang, W., Gao, H., Ma, J., Wang, H., 2020b. Geological characteristics and exploration breakthrough of shale oil in Member 3 of Shahejie Formation of Qibei subsag, Qikou sag. Acta Pet. Sin. 41 (6), 643–657 (in Chinese with English abstract).
Zhao, W., Zhu, R., Hu, S., Hou, L., Wu, S., 2020a. Accumulation contribution differences between lacustrine organic-rich shales and mudstones and their significance in shale oil evaluation. Petrol. Explor. Dev. 47 (6), 1160–1171.
Zheng, L., Qin, J., He, S., Li, G., Li, Z., 2009. Preliminary study of formation porosity thermo compression simulation experiment of hydrocarbon generation and expulsion. Petrol. Geol. Exp. 31 (3), 296–302 (in Chinese with English abstract).
Zhou, L., Chen, C., Yang, F., Cui, Y., Song, S., Guan, Q., Zhou, F., 2023. Research and breakthrough of benefit shale oil development in Cangdong Sag, Bohai Bay Basin. China Pet. Explor. 28 (4), 24-33 (in Chinese with English abstract).
Zhou, L., Zhao, X., Chai, G., Wenya, J., Pu, X., Wang, X., Han, W., Guan, Q., Feng, J., Liu, X., 2020. Key exploration & development technologies and engineering practice of continental shale oil: A case study of Member 2 of Paleogene Kongdian Formation in Cangdong Sag, Bohai Bay Basin, East China. Petrol. Explor. Dev. 47 (5), 1138–1146.